

TECHNOLOGICAL CHARACTERISTICS OF A BRICK MASONRY
STRUCTURE AND THEIR RELATIONSHIP WITH THE STRUCTURAL
BEHAVIOUR

A THESIS SUBMITTED TO
THE GRADUATE SCHOOL OF NATURAL AND APPLIED SCIENCES
OF
MIDDLE EAST TECHNICAL UNIVERSITY

BY

YASEMİN DİDEM AKTAŞ

IN PARTIAL FULFILMENT OF THE REQUIREMENTS
FOR
THE DEGREE OF MASTER OF SCIENCE
IN
ARCHAEOLOGY

SEPTEMBER 2006

Approval of the Graduate School of Natural and Applied Sciences

Prof. Dr. Canan Özgen
Director

I certify that this thesis satisfies all the requirements as a thesis for the degree of Master of Science.

Prof. Dr. Şahinde Demirci
Head of Department

This is to certify that we have read this thesis and that in our opinion it is fully adequate, in scope and quality, as a thesis for the degree of Master of Science.

Assoc. Prof. Dr. Ahmet Türer
Co-Supervisor

Prof. Dr. Emine N. Caner-Saltık
Supervisor

Examining Committee Members

Prof. Dr. Şahinde Demirci	(METU, CHEM)	_____
Prof. Dr. Emine N. Caner-Saltık	(METU, REST)	_____
Asst. Prof. Dr. Ahmet Türer	(METU, CE)	_____
Prof. Dr. Ay Melek Özer	(METU, PHYS)	_____
Prof. Dr. Ali Uzun	(METU, STAT)	_____

I hereby declare that all information in this document has been obtained and presented in accordance with academic rules and ethical conduct. I also declare that, as required by these rules and conduct, I have fully cited and referenced all material and results that are not original to this work.

Name, Last name : Yasemin Didem Aktaş

Signature :

ABSTRACT

TECHNOLOGICAL CHARACTERISTICS OF A BRICK MASONRY STRUCTURE AND THEIR RELATIONSHIP WITH THE STRUCTURAL BEHAVIOUR

Aktaş, Yasemin Didem

M.S., Department of Archaeometry

Supervisor: Prof. Dr. Emine N. Caner-Saltık

Co-Supervisor: Assoc. Prof. Dr. Ahmet Türer

September 2006, 108 pages

The aim of this study is to investigate the physical and mechanical properties of construction materials in relation with the structural behaviour of a historic structure. Within this framework, the brick masonry superstructure of Tahir ile Zühre Mescidi, a XIIIth century Seljuk monument in Konya was selected as the case study. The study started with the determination of the basic physical (bulk density, effective porosity, water absorption capacity), mechanical (modulus of elasticity, uniaxial compressive strength), durability and pozzolanic properties of original brick and mortar by laboratory analysis. The obtained data was utilized as material information at the modelling of superstructure, by means of structural analysis software, SAP2000. At the modelling stage, finite element method was used and the complexity of masonry in terms of nonlinearity and heterogeneity was taken into account within practical limits. The constructed model was investigated under dead load, wind load, snow load, temperature load and earthquake load and their possible combinations. Structural investigation was continued with two scenarios

representing possible wrong restoration interventions i.e. completion of the partially collapsed superstructure with concrete and the concrete coating over superstructure. These cases were investigated under uniform and randomly distributed temperature loads.

The results approved the safety of the superstructure under normal service conditions, defined as the appropriate combinations of dead load, snow load, wind load and temperature load. The structure appeared to be safe under the earthquake load too. The analyses carried out to simulate the inappropriate restoration works demonstrated the structural damage formations at the original structure.

Keywords: Historic structure, brick masonry, dome, finite element method

ÖZ

BİR TUĞLA ÖRGÜ YAPININ TEKNOLOJİK ÖZELLİKLERİ VE BUNLARIN YAPISAL DAVRANIŞLA İLİŞKİLERİ

Aktaş, Yasemin Didem

Yüksek Lisans, Arkeometri Bölümü

Tez Yöneticisi: Prof. Dr. Emine N. Caner-Saltık

Ortak Tez Yöneticisi: Y. Doç. Dr. Ahmet Türer

Eylül 2006, 108 sayfa

Bu çalışmanın amacı bir tarihi yapıdaki yapı malzemelerinin fiziksel ve mekanik özelliklerinin yapısal duruma etkisini araştırmaktır. Bu amaç doğrultusunda, Konya’da bir 13. yüzyıl anıtı olan Tahir ile Zühre Mescidi’nin kubbe ve Türk üçgenlerini içeren tuğla örgü üst yapısı seçilmiştir. Çalışma, yığma yapıyı oluşturan özgün tuğla ve harcın fiziksel özelliklerinin (birim hacim ağırlığı, gözeneklilik, su emme kapasitesi), mekanik özelliklerinin (esneklik modülü, basınç dayanımı) dayanıklılık ve puzolanlık özelliklerinin belirlenmesi için yapılan analizlerle ile başlamıştır. Daha sonra elde edilen bu veriler, yapının kubbe kısmının, bir yapısal analiz programı olan SAP 2000 yoluyla oluşturulmuş bilgisayar modelinde malzeme bilgisi olarak kullanılmıştır. Modelleme aşamasında sonlu elemanlar yöntemi ile malzemenin doğrusal olmayan davranışı ve heterojenliğinden kaynaklanan karmaşıklığı, pratik sınırlar dahilinde göz önünde bulundurulmuştur. Model önce, ölü yük, rüzgar yükü, kar yükü ve sıcaklık yükü ile deprem yükü ve bunların uygun kombinasyonları altında incelenmiştir. Ayrıca, kısmen yıkılan üst

yapının imento ile tamamlanması ve st yapının imento ile kaplanması gibi farklı yanlış restorasyon mdahalelerini ifade etmek zere geliřtirilen bir seri gereęe uygun senaryo ile analizlere devam edilmiřtir. Bu analizler dzgn ve kısmi yayılı sıcaklık ykleri altında incelenmiřtir. Bu analizlerde, imento ve yıęma malzeme arasındaki malzeme uyumazlıęı sebebiyle oluřan baę eksiklięi, malzemeler arasına rijit baęlantılar tanımlanarak gzetilmiřtir.

Sonuçlar yapının, l yk, rzgar yk, kar yk ve sıcaklık yk ile bunların uygun kombinasyonları řeklinde tanımlanan normal servis kořulları altında gvenli olduęunu kanıtlamıřtır. Yapının deprem yk altında da gvenli olduęu sonucuna varılmıřtır. Uygun olmayan restorasyon mdahalelerini simule etmek iin yrtlen analizlerden birkaçı, bu durumda orjinal yapıda oluřacak yapısal hasarı da aıka gstermiřtir.

Anahtar kelimeler: Tarihi yapı, tuęla rg, kubbe, sonlu elemanlar yntemi

TABLE OF CONTENTS

ABSTRACT	iv
ÖZ	vi
TABLE OF CONTENTS	viii
LIST OF TABLES	xi
LIST OF FIGURES.....	xii
LIST OF FIGURES.....	xii
CHAPTER	
1. INTRODUCTION.....	1
1.1 General Aspects of Brick Masonry	1
Physical Characteristics of Masonry	2
1.1.1.1 Masonry Units	3
1.1.1.2 Mortar	4
Mechanical Characteristics of Masonry	5
Mathematic Modelling of Masonry.....	7
1.2. Previous Studies on the Characteristics of Brick Masonry	10
1.2.1 The Studies Focused on Material Investigation	10
1.2.2 The Studies Focused on Structural Investigation.....	13
1.2 Brief History of Konya and 13 th Century Domed Masjids in / around Konya 16	
1.3 Brief History of Tahir ile Zühre Mescidi	19
1.4 Aim and Scope of the Study.....	20
2. MATERIALS, METHODS AND ANALYSES	22
2.1 Description of Samples	22
2.2 Basic Physical Properties	24

2.2.1 Effective porosity	24
2.2.2 Bulk Density.....	26
2.2.3 Water Absorption Capacity	28
2.3 Basic Mechanical Properties	30
2.3.1 Modulus of Elasticity	30
2.3.2 Uniaxial Compressive Strength.....	33
2.3.3 Durability Features	36
2.4 Pozzolanic Activity Measurements by EDTA Titration	38
2.5 Discussion of Results	41
2.6 Tensile Strength Value	46
3. STRUCTURAL INVESTIGATION.....	48
3.1 Physical Description of the Upper Structure of Tahir ile Zühre Mescidi	48
3.2 Safety of a Structure	50
3.3 Dome as a Structural Form.....	50
3.4 Derivation of Mechanical Data to be Used in Structural Analyses.....	51
3.5 Dome Behaviour in General.....	55
3.6.1 Structural Behaviour of the Upper Structure under Dead Load.....	59
3.6.2 Structural Behaviour of the Upper Structure under a Combination of Dead Load, Snow Load and Wind Loads	61
3.6.3 Structural Behaviour of the Upper Structure under Temperature Load..	65
3.6.4 Structural Behaviour of the Upper Structure under Earthquake Load	68
3.6.5 Partially Collapsed Masonry Superstructure Completed Using Concrete, Analysed under Dead Load	72
3.6.6 Partially Collapsed Masonry Superstructure Completed Using Concrete, Analysed under a Combination of Dead Load and Uniform Temperature Load of 40°C.....	74
3.6.7 Partially Collapsed Masonry Superstructure Completed Using Concrete, Analysed under a Combination of Dead Load and Randomly Distributed Temperature Load of 25°C	76

3.6.8 10 cm Thick Concrete Coating over Superstructure Analysed under a Combination of Dead Load and Uniform Temperature Load of 40°C.....	77
3.6.9 10 cm Thick Concrete Coating over Dome Only under a Combination of Dead Load and Uniform Temperature Load of 40°C.....	84
3.6.10 10 cm Thick Concrete Coating over Superstructure under a Combination of Dead Load and Randomly Distributed Temperature Load of 25°C.....	90
4. SUMMARY AND CONCLUSION.....	95
REFERENCES.....	103

LIST OF TABLES

Table 1 General information about the studied samples	23
Table 2 Effective porosity values (% volume) of the samples.....	25
Table 3 Bulk density values (g/cm ³) of the samples	27
Table 4 Water absorption capacity values (% weight) of the samples.....	29
Table 5 Modulus of elasticity values of the samples in dry and wet states (MPa) ..	32
Table 6 Uniaxial compressive strength values of the samples in dry and wet states (MPa).....	35
Table 7 Durability features of the samples.....	37
Table 8 Pozzolanic activity values (Δ EC) of the samples.....	40
Table 9 Resultant average values for physical properties (effective porosity, bulk density and water absorption capacity WAC) and modulus of elasticity (as average \pm standard deviation).....	42
Table 10 Resultant average values for uniaxial compressive strength (UCS), pozzolanicity and durability (D) (as average \pm standard deviation)	44
Table 11 Base reactions under self load.....	61
Table 12 Base reactions under self load, snow load and wind load.....	63
Table 13 Base reactions under temperature load and dead load	68

LIST OF FIGURES

Figure 1 A general view of Tahir ile Zühre Mescidi.....	20
Figure 2 Variation in porosity values (% volume) of the samples.....	26
Figure 3 Variation in bulk density values (g/cm ³) of the samples	28
Figure 4 Variation in water absorption capacity values (% weight) of the samples	30
Figure 5 Variation in modulus of elasticity (Young's Modulus) values (MPa) of the samples in dry and wet state (dry and wet states are shown by blue and pink lines, respectively).....	33
Figure 6 Correlation Developed Between Emod and UCS values Reported in Tuncoku, 2001.....	34
Figure 7 Variation in uniaxial compressive strength values (MPa) of the samples in dry and wet state (dry and wet states are shown by blue and pink lines, respectively).....	36
Figure 8 Variation in durability features of the samples.....	38
Figure 9 Variation in pozzolanic activity values (Δ EC) of the samples	41
Figure 10 Dome of Tahir ile Zühre Mescidi	49
Figure 13 Local axes directions and corresponding stress directions used in this study	57
Figure 14 3D view and top view of the model of the upper structure of Tahir ile Zühre Mescidi	58
Figure 15 3D view of SMAX diagram of the upper structure of the monument under dead load	59
Figure 16 Bottom view of SMAX diagram of the upper structure of the monument under dead load	60
Figure 17 3D SMAX diagram of the upper structure of the monument under the combination of its dead load, snow load and wind load	62
Figure 18 3D deformed and bottom view SMAX diagram of the upper structure of the monument under wind load.....	63

Figure 19 3D and bottom views SMAX diagram of the upper structure of the monument under snow load	64
Figure 20 Applied temperature load of 25°C. Dark blue indicates the part warmer.	65
Figure 21 3D SMAX diagram of the upper structure of the monument under the combination of dead load and temperature load	66
Figure 22 3D SMAX diagrams of the upper structure of the monument under temperature load.....	67
Figure 23 Top and bottom views of SMAX diagram of the upper structure of the monument under temperature load.....	68
Figure 24 Response spectrum according to ABYYHY 98 (Turkish Earthquake Resistant Design Code 1998) for the soil type Z4	69
Figure 25 3D deformed shape of the upper structure of the monument under the combination of earthquake load and dead load.....	70
Figure 26 3D and bottom views of S11 diagram of the upper structure of the monument under earthquake load	70
Figure 27 3D and bottom views of S22 diagram of the upper structure of the monument under earthquake load	71
Figure 28 3D and bottom views of S12 diagram of the upper structure of the monument under earthquake load	71
Figure 29 3D and bottom views of S13 diagram of the upper structure of the monument under earthquake load	72
Figure 30 3D undeformed and deformed views of the upper structure of the monument, partially collapsed and completed using concrete, under dead load (red and blue demonstrate masonry and concrete materials, respectively)	73
Figure 31 3D and bottom SMAX diagrams of the upper structure of the monument, partially collapsed and completed using concrete, under dead load	74
Figure 32 3D and bottom SMAX diagrams of the upper structure of the monument, partially collapsed and completed using concrete, under dead load and 40°C uniform temperature load	75
Figure 33 3D and bottom SMAX diagrams of the upper structure of the monument,	

partially collapsed and completed using concrete, under dead load and 25°C randomly distributed temperature load	76
Figure 34 3D and bottom views of the upper structure of the monument composed of two layers connected with rigid links	78
Figure 35 Graphs of minimum and maximum V2 and V3 values (i.e. shear forces in the 1-3 and 1-2 planes respectively) as a function of moment of inertia.	79
Figure 36 Bottom view of resulting SMAX diagrams of the upper structure of the monument with and without concrete cover, respectively, under dead load and uniformly distributed temperature load of 40°C for $I=10^{10} \text{ mm}^4$	80
Figure 37 Graphs of resulting V2 and V3 values (i.e. shear forces in the 1-3 and 1-2 planes respectively) under dead load and uniformly distributed temperature load of 40°C for $I=10^{10} \text{ mm}^4$	81
Figure 38 Critical frame elements indicated on the upper structure of the monument, covered with concrete coating, under dead load and uniformly distributed temperature load of 40°C for $I=10^{10} \text{ mm}^4$	81
Figure 39 3D and bottom views of the SMAX diagram the upper structure of the monument covered with concrete coating, under dead load and uniformly distributed temperature load of 40°C for $I=10^5 \text{ mm}^4$	82
Figure 40 Critical frame elements indicated on the upper structure of the monument, covered with concrete coating, under dead load and uniformly distributed temperature load of 40°C for $I=10^5 \text{ mm}^4$	83
Figure 41 A 3D view of the upper structure of the monument composed of two layers connected only at the dome part with rigid links.....	84
Figure 42 Graphs of minimum and maximum V2 and V3 values (i.e. shear forces in the 1-3 and 1-2 planes, respectively) as a function of moment of inertia.	85
Figure 43 3D and bottom views of the SMAX diagram the upper structure of the monument, whose dome covered with concrete coating, under dead load and uniformly distributed temperature load of 40°C for $I=10^9 \text{ mm}^4$	86
Figure 44 Bottom view of the SMAX diagram of the upper structure of the monument covered with concrete coating, under dead load and uniformly	

distributed temperature load of 40°C for $I=10^9 \text{ mm}^4$	87
Figure 45 Graphs of resulting V2 and V3 values (i.e. shear forces in the 1-3 and 1-2 planes respectively) under dead load and uniformly distributed temperature load of 40°C for $I=10^9 \text{ mm}^4$	88
Figure 46 3D bottom views of the SMAX diagram the upper structure of the monument, whose dome covered with concrete coating, under dead load and uniformly distributed temperature load of 40°C for $I=10^5 \text{ mm}^4$	89
Figure 47 Critical frame elements indicated on the upper structure of the monument, whose dome covered with concrete coating, under dead load and uniformly distributed temperature load of 40°C for $I=10^5 \text{ mm}^4$	89
Figure 48 Graphs of minimum and maximum V2 and V3 values (i.e. shear forces in the 1-3 and 1-2 planes with square and diamond markers, respectively) as a function of moment of inertia	90
Figure 49 Bottom view of the SMAX diagram of the upper structure of the monument covered with concrete coating, under dead load and randomly distributed temperature load of 25°C for $I=10^{10} \text{ mm}^4$	91
Figure 50 3D SMAX diagrams of the upper structure of the monument covered with concrete coating, under dead load and randomly distributed temperature load of 25°C for $I=10^{10} \text{ mm}^4$	92
Figure 51 Critical frame elements indicated on the of the upper structure of the monument, covered with concrete coating, under dead load and randomly distributed temperature load of 25°C for $I=10^{10} \text{ mm}^4$	92
Figure 52 3D and bottom views of resulting SMAX diagrams of the superstructure covered with concrete coating, under dead load and randomly distributed temperature load of 25°C for $I_{\text{sys}}=10^7 \text{ mm}^4$ and $I_{\text{cr.frames}}=10^6 \text{ mm}^4$	93

CHAPTER 1

INTRODUCTION

The structural behaviour of a monument is closely related with its material properties. Therefore recently, studies on the structural behaviour of historic masonry monuments based on materials' properties have gained further importance. The aim of these studies in general is to investigate the structural behaviour taking the material characteristics into consideration in a realistic manner both physical and mechanical, as well as compositional point of view, whenever applicable.

1.1 General Aspects of Brick Masonry

Masonry is simply an assemblage of stones or bricks, fired or non-fired together with mortar (Heyman, 1995: 12). It is one of the oldest construction techniques that have been used throughout the history. Mudbrick masonry is the oldest form of masonry and goes back to as early as 6000 B.C. Between 2500-2000 B.C., the clay material was started to be fired to obtain a more durable and water proof material and so, especially in some regions with abundant raw material sources, for example in Middle East, India and Africa, masonry architecture based on brick has been developed, ziggurats in Mesopotamia being the most famous and complex example. Roman brick architecture is another one worth to mention. Fired brick was continued to be used for public buildings and temples (Lu *et al.*, 2005: 909; Moropoulou *et al.*, 2005: 295, 296; Plumridge *et al.*, 1993: 10-18; Davey, 1961: 65-75). As the other main component of masonry, mortar has a long history as well. In

ancient Egypt, mud with brick masonry and gypsum with stone masonry were used. Babylonians and Assyrians also used mud mortar with or without the addition of chopped straw and reeds. The use of lime mortars and the pozzolanic lime mortars in stone and brick masonry was successfully practiced by Romans as described by Vitruvius (Davey, 1961: 120-127).

Brick masonry has been (and still is) one of the most popular construction materials due to its advantageous characteristics including economy, durability, heat insulation characteristics, and sufficient compressive strength (Lu *et al.*, 2005: 909). It offers a variety of shape, size and colour, therefore flexible plan forms and spatial compositions, which render it preferable in terms of architectural design (Hendry, 2001: 323; Plumridge *et al.*, 1993: 76). Brick is less dense and therefore lighter in comparison with stone of the same mechanical resistance. In addition, its composition is controllable to have a homogeneous material (Giuliani, 1990:155).

A limiting factor for brick, however, is its low tensile strength, which could cause serious problems at the existence of considerable lateral forces, such as heavy wind loads, earthquake, significant differential settlements, and/or nonuniform stress distribution, which create buckling effect etc. (Lu *et al.*, 2005: 909; Mele *et al.*, 2003: 355; Hendry, 2001: 323; Binda, 1997: 122-132; Heyman, 1995: 12-14; Heyman, 1982: 30).

Physical Characteristics of Masonry

Masonry is a general term used for bearing wall construction type in which the weight of the structure is carried by the walls. The term masonry describes composite materials that are quite different from each other in terms of (a) components, (b) assemblage, and (c) technique of construction (Binda *et al.*, 2000:

229) but in general, it is basically composed of masonry units, such as brick and stone blocks, and a binder, which is generally of lime or gypsum mortar at historic structures.

1.1.1.1 Masonry Units

Masonry can be classified very roughly as stone and brick masonry that reveal different characteristics and different structural behaviour, depending on different construction techniques. That classification corresponds exactly to another possible classification: masonry made of natural materials and that of artificial materials. For the former group (stone masonry), it was possible to use the stone pieces naturally formed with atmospheric agents, as well as artificially obtained ones by breaking the pieces at the site. Adobe and fired bricks can be used to make brick masonry and their composition depends mainly on the available raw material. Throughout the history, different recipes have been proposed, among the ancients of which Vitruvius is a very famous one giving detailed recipes for brick making (Giuliani, 1990:147-152).

Another factor affecting the quality of the fired bricks, besides the paste, was the firing process. Normally, the bricks were fired differently according to their position at the kiln. Those in a direct contact with the fire became very hard and fragile and did not bond well with mortar. The ones not fired well were very pale in colour. These were normally used for the provisory works and for the *caementa* (Giuliani, 1990:155).

1.1.1.2 Mortar

Mortar is mainly composed of binder and aggregate. At historic structures, the binders that were most commonly used are hydraulic or aerial lime and gypsum; but clay, bitumen, chalk etc. were also used (Zucchini *et al.*; 2004: 917). Lime mortar has been used since the fifth century in Anatolia, Syria, Cyprus and Greece. The cycle of lime is as follows:

$CaCO_3 \rightarrow CaO + CO_2$ (with the temperature applied in the kiln, limestone changes to be *quick lime*, CaO, freeing the carbon dioxide equal to approximately 44% of the initial weight)

$CaO + H_2O \rightarrow Ca(OH)_2$ (then, quicklime is mixed with water to obtain a workable putty with a process during which the resulting heat reaches even to 300°C)

$Ca(OH)_2 + CO_2 \rightarrow CaCO_3 + H_2O$ (After the application, the putty reacts with the carbon dioxide of the air, it turns again to be a limestone) (Giuliani, 1990:160, 161).

Aggregate is used to prevent cracking during drying. The most frequently used aggregates are sand, crushed stone, and crushed brick etc. However, in most cases, some organic and/or inorganic additives are used as well to improve the physical and mechanical properties of mortar, such as egg whites and yolks, blood, beer, urine, sepiolite, metakaolin and so on.

Another possible additive is ‘pozzolanic material’, that improves the hydraulicity of mortar. Pozzolanic materials can interact with lime and form insoluble products with binding properties. Therefore, they are used also to improve the mortar in terms of its adhesion, and workability as well as to provide hardening under water. The most common forms of pozzolanic materials are crushed bricks, potteries, and

fragments from tiles, that are artificial pozzolans used mostly during the Byzantine and Ottoman periods. The Romans, however, used mostly natural pozzolans, such as volcanic ash and Santorin earth, which was used firstly by Greeks. At historic structures pozzolanic mortars were used in cisterns, wells, aqueducts etc. since they were to be water resistant (Morolopou *et al.*, 2005: 295-297; Morolopou, *et al.*, 2004: 1; Baronio *et al.*, 1997: 41; Morolopou *et al.*, 1997: 119; Morolopou *et al.*, 1993: 415; Bugini *et al.*, 1993: 386, 387; Giuliani, 1990: 165). The analyses and classification of ancient masonry materials in terms of raw materials, pozzolanicity, and composition cover a big area of research in the literature.

The choice of binder and aggregate depends on the environmental availability of materials, as well as the environmental factors that the building is expected to be exposed to, the function of structure, etc.

Mechanical Characteristics of Masonry

Masonry is a composite material, which is commonly heterogeneous and non-linear in property. Therefore, the difficulty of investigating masonry from mechanical point of view is that even if the mechanical properties of the components of masonry, i.e. brick and mortar, are determined by laboratory analyses, it is hard to extrapolate those into the strength of masonry itself. Yet, it should be noted that it is easier for brick masonry than for stone masonry, owing to existing codes and standards suggesting different methods of extrapolation (Binda *et al.*, 1997: 113). Moreover, for the case of an existing historic monument, the mechanical properties of brick and mortar, composing masonry, are inevitably determined through taken samples, which are normally not in sufficient amount, and that do not have standard test size and shape. For this reason, it is generally required to use conversion formulas to reach to a standard value. However, since masonry is not homogeneous,

taking representative samples is also a difficult task (Binda *et al.*, 1997: 113, 114), as well as taking large number of samples to render the results of analyses statistically explanatory (Binda *et al.*, 2000: 210).

Furthermore, most of the non-destructive tests that can be applied *in situ* are mainly for the detection of physical characteristics (Binda *et al.*, 2000: 201). Therefore, carrying out laboratory analyses is inevitable, but these laboratory studies should always be supported with *in situ* investigation (Binda *et al.*, 1997, 116).

It has been proven that the masonry structures at which hydraulic mortars were used are more durable in comparison to the others, under static and dynamic stresses as well as environmental conditions (Moropoulou, 2004:1; Moropoulou, 2002: 543).

Geometry and the characteristics of texture as a whole (single/multiple leaf, connections, joint dimensions, distribution of masonry blocks and mortar joint arrangement etc.) play important role as well on the structural behaviour and durability of masonry (Guinea *et al.*, 2000: 731). The exact geometry of masonry is generally not known for the whole building; moreover, the mechanical properties of the composite material, as well as the properties of components, i.e. brick and mortar can be scattering throughout the building. The knowledge on the existing damage caused by the environment throughout the life of a monument is not fully known either. All these may render the assessment of structure behaviour misleading (Lourenço, 2005: 634; Zucchini, 2004: 917; Mele *et al.*, 2003: 355, 356; Binda, 1997, 115) if not supported with an extensive material investigation.

When the stress distribution of a masonry structure is investigated in an overall manner, it can ideally be said that masonry has a compressive strength, which is generally far higher than the compressive stress normally caused within the section under usual loading (this statement does not include possible local concentrations) (Heyman, 1995: 13, 14). The tensile strength of masonry is accepted to be quite

low; at most studies it is even assumed that masonry has no tensile strength, again as an ideal condition (Lu *et al.*, 2005: 909; Mele *et al.*, 2003: 355; Hendry, 2001: 323; Binda, 1997: 122-132; Heyman, 1995: 12-14; Heyman, 1982: 30).

Mathematic Modelling of Masonry

Masonry structures, due to their non-homogeneity, anisotropy, asymmetry in tension and compression, and non-linearity in compression, which are caused by the presence of mortar joints in both directions as well as building blocks themselves, require a special method of modelling and analysis (Lu *et al.*, 2005: 909; Mele *et al.*, 2003: 357; Giordano *et al.*, 2002: 1057, 1058; Binda *et al.*, 1997: 139). Although, there are a large number of analytical continuous solutions for unreinforced masonry structures, they were obtained either for a particular combination of support and load conditions or are overcomplicated. Therefore, numerical discrete approaches are needed to solve more complicated problems using multiple parameters (Lu *et al.*, 2005: 910). The numerical modelling is, however, hard to calibrate and validate because of the lack of a complete experimental data on masonry (Giordano *et al.*, 2002: 1057, 1059). The most commonly used computer programs in the literature are ABAQUS, Visual CASTEM, UDEC, ANSYS, DIANA, SAP 2000 etc.

Modelling the mortar-bed joints is another problem arising during the structural analysis of masonry. There are principally three different approaches to model the joints: (1) detailed micromodelling (discontinuous element modelling), (2) simplified micromodelling (discrete element modelling) and (3) macromodelling (smeared joint) (Lu *et al.*, 2005: 909; Zucchini *et al.*, 2004: 918). Another classification as (1) micro (two-material approach) and (2) macromodelling (equivalent-material approach), can be made as well, where micromodelling

includes discontinuous and discrete methods (Giambanco *et al.*, 2001: 6494; Giordano *et al.*, 2002: 1058).

According to the first classification, the first approach requires a consideration of mortar and masonry units as continuum, and of interfaces as discontinuum. For detailed micromodelling, it is necessary to use the characteristics and stress-strain relation of both mortar and masonry units. The difficulty of discontinuous element modelling is the necessity to provide a strict compatibility between the block mesh and joint mesh (Lu *et al.*, 2005: 910, 911; Giordano *et al.*, 2002: 1058). Second approach, on the other hand, provides a modelling independent of the characteristics of mortar. The joints function just like potential crack paths, by modelling them as large displacement lines, whereas modelling the block as small displacement areas (Lu *et al.*, 2005: 910; Giordano *et al.*, 2002: 1058). Masonry units should be enlarged in dimension to provide the geometry remaining unchanged (Lu *et al.*, 2005: 910; Zucchini *et al.*, 2004: 918). Therefore, in both methods, more or less the actual geometry of the structure is followed, bringing about the complexity of the model. Moreover, generally the actual distribution of masonry is not visible due to finishing materials such as plasters (Giordano *et al.*, 2002: 1068). Another tricky point with these approaches is to reflect at the model that any sliding at joint could propagate cracks (Giordano *et al.*, 2002: 1058).

In the third approach, called smeared joint method, a homogenization process is carried out and therefore whole composite material is seen as a continuum whose properties are an average of those of masonry unit and mortar (Lu *et al.*, 2005: 910; Zucchini *et al.*, 2004: 918, Binda, 1997: 139). The choice of the technique for modelling joints should depend on the content of the project and, therefore on the required grade of refinement (Lu *et al.*, 2005: 910; Guinea *et al.*, 2000: 731). However, it can be said roughly that the usage of macromodelling is common, efficient, simple, and in general sufficiently accurate (Lu *et al.*, 2005: 910; Giordano *et al.*, 2002: 1058). When the entire structure is to be modelled, generally

this easier method of homogenisation is preferred because with the two-material approach the model would have a very large size and complexity (Giordano *et al.*, 2002: 1057, 1058). Yet, it should not be forgotten that, smeared joint method bypasses the actual physics of the problem. Particularly after the tension resistance is reached, it is generally hard to reflect the geometry change due to large cracks by using this approach, because its properties average the effect of cracked and uncracked material within the element (Martini, 1998: 130). As a result, assessing the failure of masonry by this method is an insufficient approximation. This can be clearly seen when a numerical analysis and an experimental test are conducted at the same time, for the same structure (Giordano *et al.*, 2002: 1061; Guinea *et al.*, 2000: 731). Besides, smeared joint approach suggests a ‘periodic structure’, which generally is not the case when historic structures are considered. This non-periodicity includes the scattering of material characteristics of brick and mortars throughout the monument as well as the placements and dimensions of units, the thicknesses of mortars etc. (Cluni *et al.*, 2004: 1912). It is worth also to mention that in the cases where there is a big difference between the stiffness of mortar and that of masonry unit, smeared joint modelling may create a large error because this difference causes an unequal distribution of deformations between mortar and masonry unit, which cannot be reflected using this modelling method (Zucchini *et al.*, 2002: 3235-3238).

Another problem of modelling masonry is the dependency of the results on mesh. The problem of mesh dependency can be classified as mesh organization dependency and mesh size dependency, i.e. the shape and distribution of meshes throughout model and their dimensions, respectively (Giordano *et al.*, 2002: 1059, 1060).

The type of analysis of masonry structures is also important. Linear analysis does not reflect the overall behaviour of unreinforced masonry due to its high non-linearity, and yet, within the low deformation range, it gives quite accurate results

(Martini, 1998: 127, 130). The handicap of linear analysis starts with the crack propagation at high strains. Beyond this point, the change in geometry is realized simultaneously, which causes another loading situation, propagating further the change in geometry. Therefore, large displacements require an iterative solution strategy (Martini, 1997: 130).

For a constructed model of masonry structure to give reliable results, it should reflect material characteristics well. The structural theory of masonry can be better established after a detailed definition of material properties. Because the common structural action, which masonry has, “*arises directly from the properties of the material*” (Heyman, 1995: 12; Heyman, 1982: 30).

1.2. Previous Studies on the Characteristics of Brick Masonry

There are many studies that were done previously on this subject. These studies can be classified as follows:

- a) Those focused mainly on materials’ analyses,
- b) Those focused mainly on structural analyses.

1.2.1 The Studies Focused on Material Investigation

The studies carried out for the determination of the properties of construction materials of historic structures by laboratory analyses occupy a large space in the literature, some of them relating these characteristics to the structural behaviour as

well. Moropoulou *et al.* (2002) in their study on Hagia Sophia clearly declared the importance of mechanical and chemical properties of the mortar and bricks used in the masonry on the static and dynamic behaviour of structure. Study included mainly the material analyses to be able to predict the behaviour of the monument under seismic loads. Besides, Moropoulou *et al.* (2005) investigated the masonry as a 'composite material' in terms of its raw materials. This was a thorough study, which compared different types of masonry mortars, such as lime mortars, hydraulic lime mortars, natural pozzolanic mortars etc., mainly in terms of compositional properties, with a big importance attached on pozzolanicity. The study of Moropoulou *et al.* (2004) was on the pozzolanic property of historic mortars too. Within the framework of this study, an experimental work was carried out to determine the composition of pozzolanic material in detail and then the possibility of the usage of pozzolanic material in modern day applications was mentioned. In 2000, on the other hand, Moropoulou *et al.* studied on a set of Byzantine monuments in Kiev and compared them with another Byzantine set in Istanbul, which had been studied before. The investigation included the construction techniques and materials. Mechanical, mineralogical, chemical and microstructural characteristics of brick and mortar were determined both separately and in a composite manner. The similarity between these properties of the monuments in Istanbul and in Kiev was concluded. Moropoulou *et al.* (1997) worked directly on rubble stone masonry mortars which is, again, a mainly compositional investigation. The study was carried out both *in situ* and in the laboratory. The former part of the study revealed the construction characteristics of the structure, while the latter has provided information on the physical and compositional properties of mortars.

Corradi *et al.* (2003) carried out an experimental study to evaluate several mechanical properties (like shear strength and modulus of elasticity) of masonry walls. It is a thorough study on five different structures, having typical masonry walls in the Umbria region of Italy, which was composed of in-situ and laboratory parts. At the end of the study different techniques to evaluate the mechanical

properties of masonry were confronted. It was also concluded that the Italian Standard underestimate the shear strength of stone masonry.

Masonry always remained a type of material difficult to analyse. Binda *et al.* (2000) aimed to define a research procedure for historic masonry structures so that a damage assessment could be done and reliable input values could be obtained for structural analyses. It is an exhaustive study, which started with the possible non-destructive tests that can be applied to masonry to characterize masonry. It discussed 'safety' and gave basic information on behaviour of masonry. The environmental effect and effect of settlement etc. were included as well, contributing to the discussion of durability of masonry. Within this framework, the study carried out by Binda *et al.* (2002) can be seen as a partial application of the previously mentioned study. In the study case of the church of S. Nicolò l'Arena whose some structural elements got damaged by the earthquake of 1990, masonry characterization was carried out by the application of some non-destructive techniques (sonic, radar, flat-jack etc.). at the end of those applications, the different materials and building techniques used could be distinguished and a high heterogeneity in terms of these characteristics was concluded.

One of the studies that was carried out on the experimental characterization of Seljuk Period construction materials was made by Tuncoku (1993). He studied on the original brick and mortar of Tahir ile Zühre Mescidi, as well as the intervention materials added during the restoration works in a later period. In this study, the physical, mechanical, and compositional properties of raw materials were determined. A qualitative analysis of soluble salts was carried out. The compatibility between original and intervention materials was discussed. A restoration proposal was made as well based on the reached conclusions. The same author, at a later study (2001) studied 22 different Seljuk Period structures, including, again, Tahir ile Zühre Mescidi. This time, the study was concentrated especially on mortars. Physical, mechanical and compositional characterisation of

mortars was made in detail and a comparative study was carried out to conclude about the technological characteristics of 13th century Seljuk construction.

1.2.2 The Studies Focused on Structural Investigation

The structural investigation of masonry structures through their computer modelling has been attracting growing attention in recent years. In the literature, it is possible to find a great number of studies on modelling of masonry as well as experimental and analytical works, structural behaviour etc. The general aim of the studies on computer modelling of masonry is to reach to a more realistic, more detailed result in an efficient and simple manner. Cluni *et al.* (2004), for example, proposed a ‘representative volume element’ instead of the ‘periodic cell’ that is used conventionally. Therefore, the study reflected the ‘non periodicity’ of historic masonry monuments in terms of geometry and materials’ properties in a more realistic way. As mentioned before, the heterogeneity of masonry material was tried to be reflected always more and more. Zucchini *et al.* (2002) attempted to develop a novel micro-mechanical model for masonry, which took the stiffness difference between mortar and masonry unit as well. The modelling part of the work was supported strongly with analytical studies. Guinea *et al.* (2000) aimed to create a composite numerical model of brick masonry, reflecting the masonry fracture in a more detailed way than the conventional methods. For this purpose, first of all, fracture properties of material were determined. The finite element code used for modelling was ANSYS. At the end, a comparison between the numerical and experimental results has been carried out, which concluded that the method was satisfactory.

The eventual effect of different loading conditions was another factor that was tried to be simulated very often. Lu *et al.* (2005) investigated the behaviour of

unreinforced masonry walls mainly under lateral loads, both distributed and concentrated, with some modifications including eccentric vertical loading. The study has developed a solution algorithm. It is also worth to mention the study of Martini (1998), which is the initial part of a large research of investigating the masonry walls in Pompeii. Here, Martini discussed the behaviour of unreinforced masonry walls under in-plane and out-of-plane loads and modelling techniques of masonry subjected to the latter type of loading. Using the structural analysis code ABAQUS, a numerical model was created with discrete joint modelling and then, the behaviour followed by non-linear analysis of this model was compared with a theoretical and an experimental study to verify its accuracy.

Homogenization process, as mentioned before, is a characteristic rather important at the FE modelling of masonry structures. The discussion of different methods and the studies including comparative approaches, therefore, occupied always a large space in the relevant literature. Lourenço (2005) aimed to introduce a study, including damage assessment and diagnosis, as well as strengthening of a historic monument in detail. The study case was a monument in Portugal, namely Outeiro Church. For the mechanical properties of the masonry, previous studies were utilized. Then, a structural model was formed based on these characterisations, using smeared element approach and according to the results of a linear-elastic analysis, necessary measures to be taken were decided. That of Bernardeschi *et al.* (2004) is another study in which masonry modelling was discussed in terms of homogenization procedure. With two different types of approach, discrete element and smeared joint modelling, seismic vulnerability of a monument was investigated. For this study a finite element code called NOSA has been used. Giordano *et al.* (2002) carried out a study which aimed to compare different methods and software for computer modelling of masonry joints. In this study, a finite element model based on smeared joint constitutive law, another based on discontinuous element method, and a third one based on discrete element method were constructed. For these different types of analysis ABAQUS, Visual CASTEM, and UDEC

commercial codes were used, respectively. At the same time, a full-scale model of façade of the structure under investigation was constructed in the laboratory environment to support the computer studies with experimental data.

In addition to these, it is worth to mention the studies dealing with the non-linearity of masonry material with different types of analyses. Carpinteri *et al.* (2005) made a case study, through which the non-destructive evaluation tests that can be used for damage assessment of masonry were presented. The main aim of the study was to differentiate between the stable and evolving damage patterns. Using the code DIANA, a model of the monument was created, taking the presence of openings and the variation of wall thicknesses into account. Elastic and non-linear analyses were carried out, but no comment was made on which type of analysis gave more accurate results. That of Valluzzi *et al.* (2002) was another study where in situ investigation and FE modelling were together. In this study firstly, the columns of ‘Arselane’ of Venice was examined by sonic tomography to understand the level of consistency. By borehole coring, the foundation data was obtained. Then, by means of a FE model, dynamic identification was carried out. The study stressed the possibility to apply the constructed model to similar structures and to simulate possible interventions. Mele *et al.* (2003) made a study aiming to set a procedure for modelling masonry numerically as accurately as possible and to assess the monuments behaviour under seismic loads. A solution that was proposed there was to analyse firstly the whole structure in linear range through a 3D model and then, according to the weak points and the general failure mechanism obtained, to carry out a nonlinear analysis through a 2D modelling. SAP 2000 and ABAQUS were used for linear and nonlinear analyses, respectively. This study constituted a part of a wide research activity on masonry church buildings and the authors concluded, “*the analysis of a specific case study can be extrapolated, through parametric analyses carried out under appropriate hypothesis, to other significant cases and generalised for covering a wide building category*” (Mele *et al.*, 2003: 366).

1.2 Brief History of Konya and 13th Century Domed Masjids in / around Konya

Konya is a central Anatolian city. It has definitely been settled since Neolithic times (approximately 7000-6500 B.C.) like those at Çatalhöyük and Canhasan (Dülgerler, 1984: 9, Atçeken, 1998: 8). Archaeological excavations showed that Konya has been occupied also during Chalcolithic (approximately 5000-3000B.C.) and Bronze (2000-1650 B.C.) Ages. Hittites founded a civilization there between about 1650 and 712 B.C. (Karahöyük, Eflatunpınar), which is, at the same time, the first political association at Konya (Dülgerler, 1984: 9). Phrygians (712-695 B.C.) and Lydians (680-546 B.C.) followed them. For some time, Persian dominance was seen until Alexander the Great conquered Anatolia in 333 B.C. After his death at 323 B.C., first Selefkis then Bergama Kingdom had the city (Dülgerler, 1984: 9, 10; Atçeken, 1998: 9). By means of heritage, in 133 B.C. Roman Period in Konya started. (Dülgerler, 1984: 10, 11; Atçeken, 1998: 9,10). The name of the city was *Iconium* in Roman Period (Dülgerler, 1984: 9). Strabon writes that Konya was a small but important city with its role in Christianity, which had developed especially after St. Paul settled in Konya in around 47 A.D. (Dülgerler, 1984: 10; Atçeken, 1998: 9). In 395 A.D. Konya became a part of Byzantine and until 1074 it was ruled by them. *Toxovio* was the name of the city during the Byzantine Period, in Arabic sources, it was *Kûniya*.

In 1097 Konya became the capital of the state. Konya, after that date, turned to be a highly cultural centre. Political power passed to Karamanids in 1318 and to Ottomans in 1466 until the foundation of Turkish Republic (Kuran, 1980: 80-81).

Anatolian Seljuk Period had its golden age, both in terms of economic prosperity and artistic achievements during 13th century. The heydays of Anatolian Seljuks and therefore of Konya coincide especially with the period of Alaeddin Keykubad

(1219-1237). Especially in this term, in and around Konya many mosques, masjids, turbes (tombs) were constructed (Aslanapa, 1971: 119).

However it is interesting that, as Kuban mentioned, although there is just one mosque, which was constructed by the Sultan (Aleaddin Mosque), there are about 53 masjids in and near Konya. This situation somehow tells us that the Seljuk religious architecture was shaped mostly by masjids rather than mosques. It is also clear that the masjid construction tradition is a local event, since it cannot be seen in other Seljuk settlements, as much as in Konya (Kuban, 2002: 151).

These masjids show several similarities in terms of their architectural features. First of all, they are domed. They have generally a single spaced, square or rectangular plan, therefore the transition from the body walls to the dome is provided by Turkish triangles or squinches. Seljuk masjids are a step before the maturation of Ottoman architecture. The single spaced domed worship structure may have originated from tomb structures, which were constructed by Seljuks before coming to Anatolia. (Dilaver, 1970: 17). This suggestion is supported by the fact that some of the masjids under question have a part, really or symbolically separated for tombs. Tahir ile Zühre mescidi is also an example to such masjids, together with Beyhekim Mescidi in Konya and Akşebe Sultan Mescidi in Alanya. Several examples to those that have just one prayer hall and not an extra room in Konya are Hacı Ferruh Masjidi, Konya İnce Minareli Medrese Masjidi and Konya Sırçalı Masjidi.

The 13th century Seljuk masjids had minarets, which were generally higher in comparison to the height of domed prayer part. This conclusion, however, was driven from the old photos since, except one, the upper parts of all minarets belonging to this period had been collapsed (Kuran, 1980: 85)

It is a widely accepted opinion that the space other than main prayer room is a “son

cemaat mahalli”, for showing hospitality to guests as well as to people who are late for prayer or as the part used during summer (Katoğlu: 1966, 81, 87). Some of those are with open portico and some not. According to Dilaver’s point of view they are not “son cemaat mahalli” but they have a preparation function, because of that the direction of those sections are not available for prayer, Dilaver, however, agrees that these are the origin of a later “son cemaat mahalli” tradition at Ottoman architecture (Dilaver, 1970: 20-21).

At almost all masjids are in a bad state of preservation, either due to lack of attention or to wrong interventions. Many of them do not have an inscription panel, but for the masjids in Konya the construction date is considered to be more or less within 13th century (Kuban, 2002: 151).

Another common property of the masjids is their construction materials. Usual construction material of the period was stone and brick for such structures. Stone, as traditional construction material of Anatolia, can be widely seen also at Seljuk structures. Generally the walls were, up to some height, constructed with stone, either in finely cut or rubble units. To use cut stones as covering to rubble infill was also a widely used method. In Seljuk Period stone architecture, although heights of cut stones were more or less the same, widths were normally totally different from each other. It is well known that during Seljuk Period, the construction materials were provided from the vicinity because of economic reasons (Bakırer, 1994: 168).

Brick was an architectural custom that Seljuk took with them from Iran and Horasan region. In spite of the fact that during Seljuk Period brick technology had been highly developed and big achievements succeeded in terms of ornament, in Anatolia brick has always been a secondary material for construction. Brick was used at both structural and decorative elements in Seljuk Period (Bakırer, 1994: 171, Bakırer, 1972: 187). Decorative parts were either constructed together with the structure itself or covered after construction. Normal sized bricks, cut bricks of

various size and shape, glazed or non-glazed, were used (Bakırer, 1972: 187,195). At the masjid structures under investigation, the upper parts of the walls and superstructure, domes and vaults, were constructed of brick masonry.

Timber, as an auxiliary material, plays an important role at such structures. Timber beams were mainly placed horizontally inside walls, which could be both rubble stone and brick, to distribute the present stresses uniformly in horizontal direction and therefore to prevent possible cracks. If used as load bearing element or at the superstructure, then it was generally ornamented, but anyway it is hard to see the usage as a part of superstructure since timber is an easily deteriorated material (Bakırer, 1995: 174, 175).

1.3 Brief History of Tahir ile Zühre Mescidi

Tahir ile Zühre is the name, which is used mostly among people living in Konya, like several others such as Arzu ile Kanber Tekkesi, Dönbaba Tekkesi etc. According to Konyalı (1964), the name is Sahip Ata Masjidi since masjid was made by Sahip Ata Fahrettin Ali bin Hüseyin. It is located at Beyhekim Neighbourhood, at the cross section of two streets: İmam Bağavi and Muzaffer Hamit. The masjid does not have an inscription panel, therefore the construction date can just be predicted according to Sahip Ata Mosque. The mosque was constructed in 1258, therefore the date for the construction of the masjid might be close to this. As Konyalı informs us, when the masjid was inherited to Sütçü Mehmet in 1902, it was not in use (Konyalı, 1964: 517, Akmaydalı, 1982: 101). It is also known that in 1958, some interventions for the repair of the structure were carried out by Vakıflar. During those repairs, many changes were made. Masjid had been closed to worship since more than 120 years.

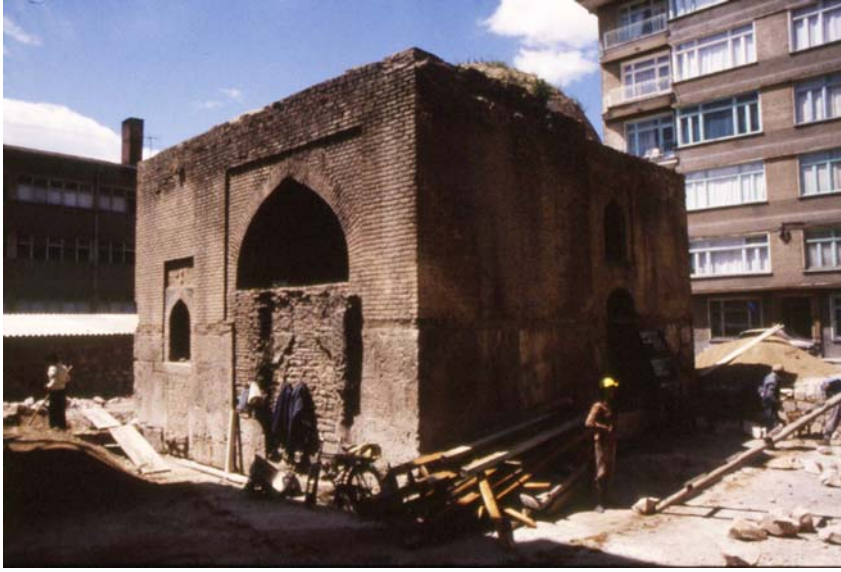


Figure 1 A general view of Tahir ile Zühre Mescidi

1.4 Aim and Scope of the Study

The studies aiming a more integrated investigation of historic structures, taking the material properties into consideration and analysing the structural behaviour in relation to them, are gaining importance recently. A reason for this is that the structural behaviour is strictly related with the material characteristics, both from physical and mechanical point of view, as well as the compositional one. In the case of historic masonry structures, with more heterogeneous and non-linear property, and subjected to atmospheric agents (and other degrading and deteriorating factors) for a long time, further big is the necessity to carry out a study including a thorough material investigation to conclude on the structural behaviour of the structure.

The aim of this study was to investigate the structural behaviour of a historic monument in relation with its material characteristics. For this purpose, Tahir ile

Zühre Mescidi in Konya, Turkey, which is a 13th century brick-masonry religious structure, namely masjid, was chosen as the case study. The study covered the investigation of the materials composing masonry, i.e. the original brick and mortar, through a series of laboratory material analyses to determine their basic physical and mechanical properties, as well as pozzolanicity.

Then, the defined materials properties were used as input at the finite element modelling phase of the superstructure, achieved by one of the commercially available software, SAP 2000. The model was first analyzed under the appropriate combinations of dead load, wind load, snow load, earthquake load and temperature load. Then, the case that the superstructure is partially collapsed and completed using concrete is tried to be investigated. In addition, a concrete coating layer was simulated over the dome and the temperature induced forces and strains at the interface were studied.

CHAPTER 2

MATERIALS, METHODS AND ANALYSES

In this study, the basic physical and mechanical properties of original materials were determined. The basic physical properties analysed are bulk density, effective porosity and water absorption capacity. The mechanical properties studied are modulus of elasticity and uniaxial compressive strength. In addition, durability characteristics and pozzolanic activity properties of the components were determined.

2.1 Description of Samples

In this study, the brick and mortar samples of Tahir ile Zühre Mescidi, in Konya that were collected during a previous study were analysed. 24 brick and 2 mortar samples representing the brick masonry upper structure were used. They were coded as follows: the first letter T indicated the name of the monument Tahir ile Zühre Mescidi, the second letter indicated the type of the material; B: brick, M: mortar and the number indicated the sample number. The brick samples were classified also according to their colours, which were determined by means of MUNSELL Soil Colour Chart (1966).

Table 1 General information about the studied samples

Sample Code	Type	Munsell Code	Colour
TB 1	Brick	2.5YR 6/6	Reddish brown
TB 2	Brick	2.5YR 6/6	Reddish brown
TB 3	Brick	2.5YR 6/6	Reddish brown
TB 4	Brick	2.5YR 6/6	Reddish brown
TB 5	Brick	2.5YR 6/6	Reddish brown
TB 6	Brick	2.5YR 6/6	Reddish brown
TB 7	Brick	2.5YR 6/6	Reddish brown
TB 8	Brick	2.5YR 6/6	Reddish brown
TB 9	Brick	2.5YR 6/6	Reddish brown
TB 10	Brick	2.5YR 6/6	Reddish brown
TB 11	Brick	2.5YR 6/6	Reddish brown
TB 12	Brick	5YR 7/4	Pale brown
TB 13	Brick	5YR 7/4	Pale brown
TB 14	Brick	5YR 7/4	Pale brown
TB 15	Brick	5YR 7/4	Pale brown
TB 16	Brick	5YR 7/4	Pale brown
TB 17	Brick	5YR 7/4	Pale brown
TB 18	Brick	5YR 7/4	Pale brown
TB 19	Brick	5YR 7/4	Pale brown
TB 20	Brick	5YR 6/4	Brown
TB 21	Brick	5YR 6/4	Brown
TB 22	Brick	5YR 6/4	Brown
TB 23	Brick	5YR 6/4	Brown
TB 24	Brick	7.5YR 6/4	Dull brown
TM 1	Mortar		
TM 2	Mortar		

In terms of the colours determined according to MUNSELL Colour Chart (1966), the bricks were categorized into four classes as reddish brown (11 samples), pale brown (8 samples), brown (4 samples) and dull brown (1 sample).

2.2 Basic Physical Properties

For the determination of basic physical properties, the samples were dried in the oven at 35°C to constant weight until the difference between two successive weighings at an interval of 24 hours, is not more than 0.1% of the sample weight (Teutonico, 1988). These weight measurements were recorded as the dry weights of the samples (m_{dry}). The samples were then saturated in distilled water in a vacuum at about 0.132 atm pressure. The weights of the water-saturated samples were recorded as saturated weights (m_{sat}). The weights of saturated samples were measured also in water and recorded as Archimedes weight (m_{arch}). They were used in the calculation of effective porosity, bulk density and water absorption capacity of the samples (RILEM, 1980).

2.2.1 Effective porosity

According to RILEM, (1980), effective porosity (P) is defined as the percentage of the total volume of a porous material occupied by pores or, more simply, the empty spaces or voids in the mass. Bulk density was calculated using the following equation:

$$P(\%volume) = [(m_{sat} - m_{dry}) / (m_{sat} - m_{arch})]$$

where, m_{sat} : saturated weight (g)

m_{dry} : dry weight (g)

m_{arch} : the weight of the sample in water (g)

The obtained results are given in Table 2 and Figure 2.

Table 2 Effective porosity values (% volume) of the samples

Samples	P (% volume)
Bricks	
Reddish brown	
TB 1	52
TB 3	52
TB 4	50
TB 5	50
TB 6	52
TB 7	52
TB 8	52
TB 9	47
TB 10	48
Pale brown	
TB 12	52
TB 13	52
TB 16	53
TB 17	50
TB 18	49
TB 19	53
Brown	
TB 20	47
TB 21	44
TB 22	42
TB 23	45
Dull brown	
TB 24	32
Mortars	
TM 1	42
TM 2	39

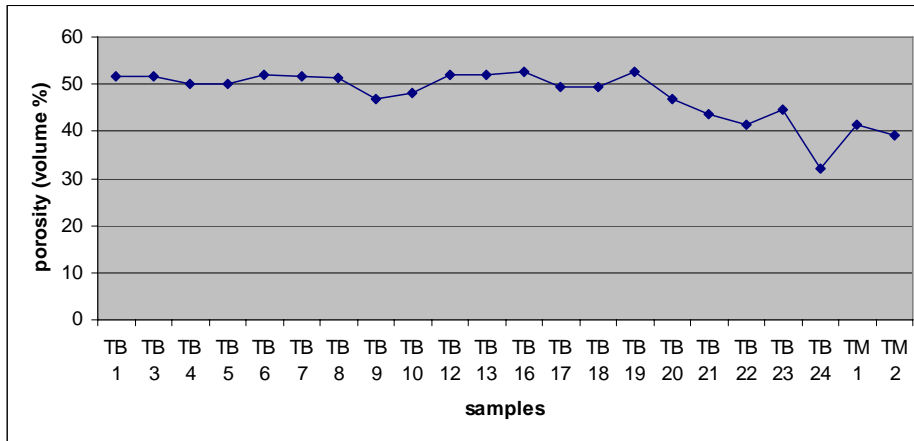


Figure 2 Variation in porosity values (% volume) of the samples

2.2.2 Bulk Density

Bulk density (D) is the ratio of the mass to the bulk volume of the sample (RILEM, 1980) and is formulated as follows:

$$D(g / cm^3) = m_{dry} / (m_{sat} - m_{arch})$$

where, m_{sat} : saturated weight (g)

m_{dry} : dry weight (g)

m_{arch} : the weight of the sample in water (g)

The obtained results are given in Table 3 and Figure 3.

Table 3 Bulk density values (g/cm³) of the samples

Samples	D (g/cm ³)
Bricks	
Reddish brown	
TB 1	1.34
TB 3	1.33
TB 4	1.35
TB 5	1.34
TB 6	1.32
TB 7	1.31
TB 8	1.34
TB 9	1.38
TB 10	1.43
Pale brown	
TB 12	1.35
TB 13	1.34
TB 16	1.33
TB 17	1.42
TB 18	1.42
TB 19	1.31
Brown	
TB 20	1.44
TB 21	1.49
TB 22	1.52
TB 23	1.49
Dull brown	
TB 24	1.78
Mortars	
TM 1	1.49
TM 2	1.57

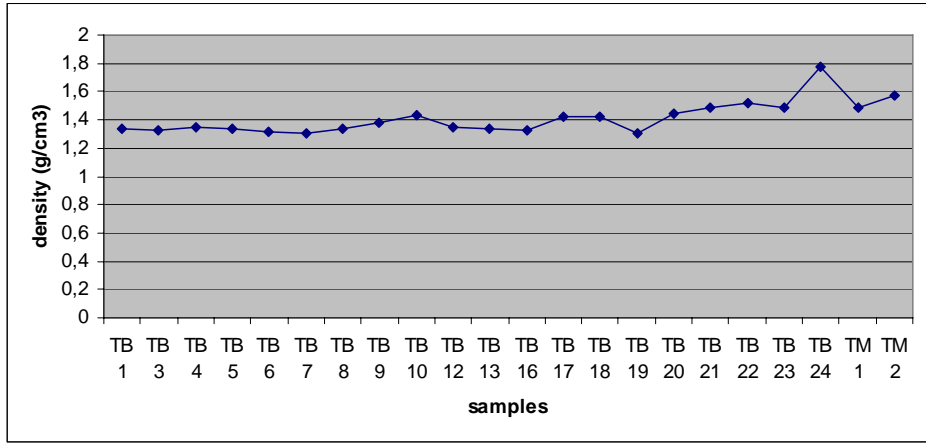


Figure 3 Variation in bulk density values (g/cm³) of the samples

2.2.3 Water Absorption Capacity

Water absorption capacity (WAC) is the maximum amount of water that material can absorb. According to RILEM (1980), water absorption capacity is formulated as follows:

$$WAC(\%weight) = (m_{sat} - m_{arch}) / m_{arch}$$

where, m_{sat} : saturated weight (g)

m_{arch} : the weight of the sample in water (g)

The obtained results are given in Table 4 and Figure 4.

Table 4 Water absorption capacity values (% weight) of the samples

Samples	WAC (%)
Bricks	
Reddish brown	
TB 1	39
TB 3	39
TB 4	37
TB 5	37
TB 6	39
TB 7	39
TB 8	38
TB 9	34
TB 10	34
Pale brown	
TB 12	39
TB 13	39
TB 16	40
TB 17	35
TB 18	35
TB 19	40
Brown	
TB 20	32
TB 21	29
TB 22	27
TB 23	30
Dull brown	
TB 24	18
Mortars	
TM 1	28
TM 2	25

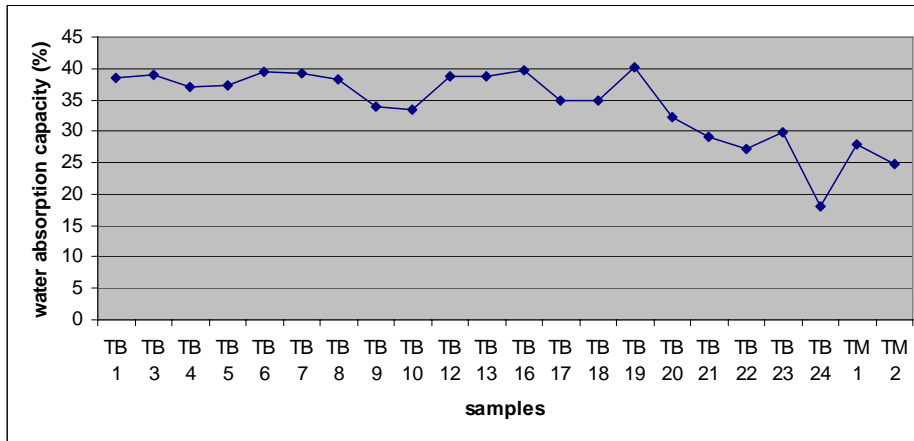


Figure 4 Variation in water absorption capacity values (% weight) of the samples

2.3 Basic Mechanical Properties

Investigation of basic mechanical properties in this study involved the determination of modulus of elasticity, uniaxial compressive strength and durability features of the samples.

2.3.1 Modulus of Elasticity

Modulus of elasticity (E_{mod}) is defined as the slope of the elastic portion of stress-strain curve, which is drawn according to the stresses and the deformation of the material. It is an indication of deformation capacity of the material.

The modulus of elasticity was determined by ultrasonic pulse velocity measurements (ASTM D 2845-90; RILEM, 1980). For this purpose, a pulse generating test equipment, PUNDIT*plus*, with its probes, transmitter and receiver of 220 kHz, was used. This method was based on the measurement of the required time for the ultrasonic waves to transverse the cross section of the test specimen. The velocity of the waves was calculated by using the following formula (ASTM D 2845-90; RILEM, 1980):

$$V = l / t$$

where, V: ultrasonic velocity (mm / s)

l: the distance travelled by the wave (cross section of test specimen) (mm)

t: travel time (s)

The modulus of elasticity was then obtained through the bulk density of the specimen and ultrasonic velocity by the following expression (RILEM, 1980)

$$E_{\text{mod}} = D * V^2 (1 + \nu_{\text{dyn}})(1 - 2\nu_{\text{dyn}}) / (1 - \nu_{\text{dyn}})$$

where, E_{mod} : modulus of elasticity ($\text{N/m}^2 = \text{Pa}$)

D: bulk density of the specimen (kg/m^3)

V: wave velocity (m/s) (Ultrasonic velocities were measured for all three dimensions of the sample prism and three measurements were taken for each dimension. At the end, the average of nine values was accepted as wave velocity)

ν_{dyn} : Poisson's ratio (Poisson's ratio is the ratio of transverse contraction strain to longitudinal extension strain in the direction of stretching force. Poisson's ratio was taken as 0.20 in the calculations here, since it is a commonly accepted value in the literature for historic masonry material (Carpinteri et al., 2005: 391, Ramos et al., 2004: 1298))

The experiment was carried out for both dry and saturated states of the samples.

The results are given at Table 5 and Figure 4.

Table 5 Modulus of elasticity values of the samples in dry and wet states (MPa)

Bricks	E _{mod} (MN/m ²)	
	DRY	WET
Reddish brown		
TB 1	937	729
TB 3	1381	780
TB 4	855	569
TB 5	684	560
TB 6	997	559
TB 7	765	686
TB 8	881	846
TB 9	1139	1051
Pale brown		
TB 12	1263	901
TB 13	1097	892
TB 16	913	630
TB 17	1714	1249
TB 18	1156	984
TB 19	845	554
Brown		
TB 20	1504	1094
TB 21	1748	1372
TB 22	1878	1651
Dull brown		
TB 24	1440	1408
Mortars		
TM 1	1124	911
TM 2	528	457

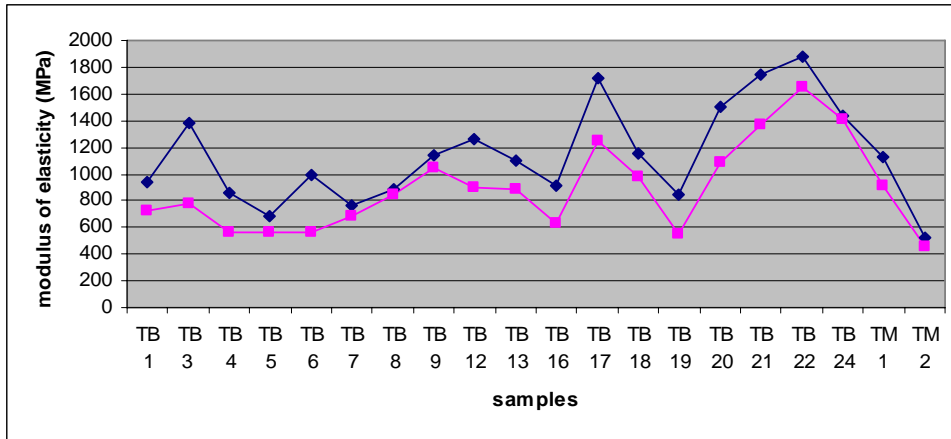


Figure 5 Variation in modulus of elasticity (Young’s Modulus) values (MPa) of the samples in dry and wet state (dry and wet states are shown by blue and pink lines, respectively).

2.3.2 Uniaxial Compressive Strength

In this study, in addition to the laboratory analyses explained above, the results of a previous study carried out by Tuncoku (Tuncoku, 2001) were used as well to obtain the uniaxial compressive strength values of the samples studied here. The mentioned study included the uniaxial compressive strength investigation carried out by point load testing, as well as the determination of modulus of elasticity values through ultrasonic velocity measurements for a wide range of mortar samples taken from 22 different Seljuk Period structures. Therefore, utilizing these values, a search for any correlation between uniaxial compressive strength versus modulus of elasticity was made (Figure 6).

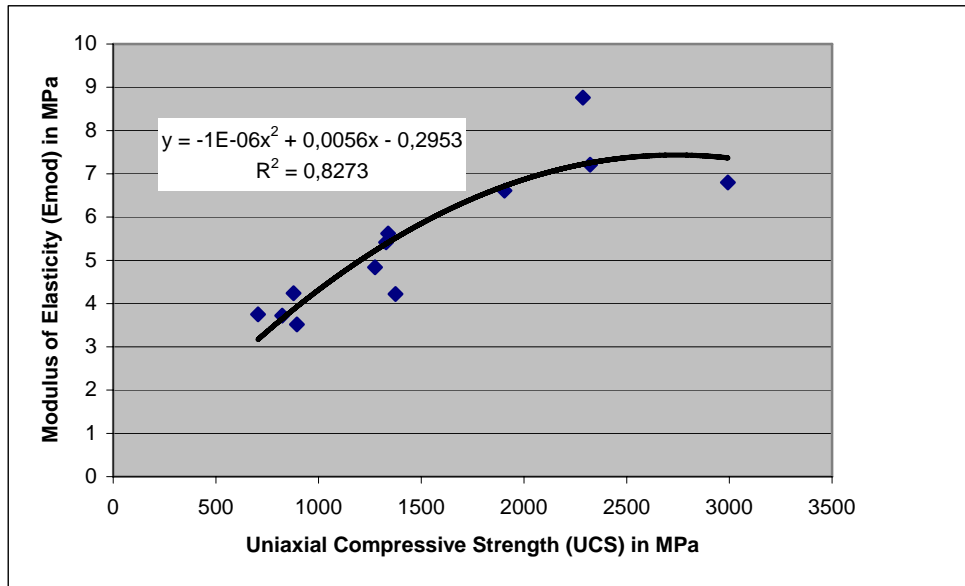


Figure 6 Correlation Developed Between Emod and UCS values Reported in Tuncoku, 2001

The best second degree equation representing the relation between the modulus of elasticity and uniaxial compressive strength values was tried to be found. The reason for this is that the value in such an equation for concrete is two, as seen below:

$$UCS = 2.105 * 10^{-4} (E_{mod})^2 \quad (\text{Ersoy, 1994: 26})$$

where, both E_{mod} and UCS are in MPa.

The equation developed to be used for obtaining the uniaxial compressive strength values of the original brick and mortar materials of Tahir ile Zühre Mescidi is given below:

$$UCS = -10^{-6}(E_{\text{mod}})^2 + 0.0056(E_{\text{mod}}) - 0.2953$$

where, both E_{mod} and UCS are in MPa.

The uniaxial compressive strength values calculated according to this equation (using the results of the previous analysis, wet and dry moduli of elasticity of the samples) are shown in Table 6 and Figure 7.

Table 6 Uniaxial compressive strength values of the samples in dry and wet states (MPa)

	UCS (MPa)	
Bricks	DRY	WET
Reddish brown		
TB 1	5.8	4.3
TB 3	9.4	4.7
TB 4	5.2	3.2
TB 5	4.0	3.2
TB 6	6.3	3.2
TB 7	4.6	4.0
TB 8	5.4	5.2
TB 9	7.4	6.7
Pale brown		
TB 12	8.4	5.6
TB 13	7.1	5.5
TB 16	5.7	3.6
TB 17	12.3	8.3
TB 18	7.5	6.2
TB 19	5.2	3.1
Brown		
TB 20	10.4	7.0
TB 21	12.6	9.3
TB 22	13.8	11.7
Dull brown		
TB 24	9.8	9.6
Mortars		
TM 1	7.3	5.6
TM 2	2.9	2.5

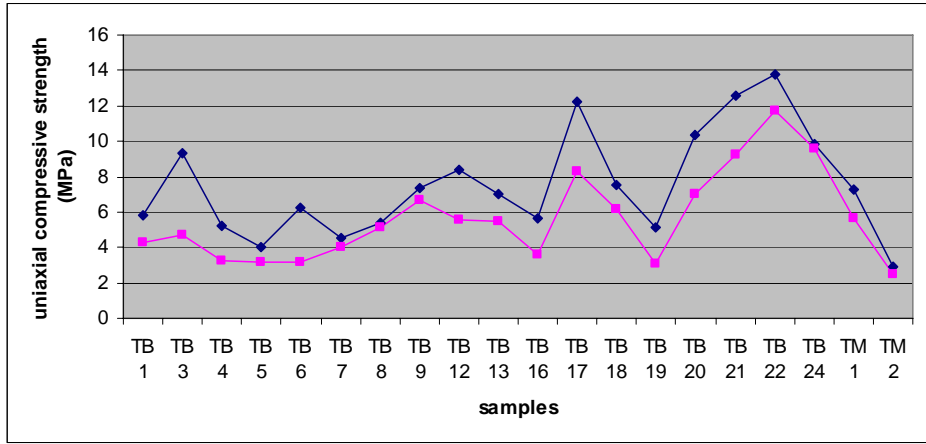


Figure 7 Variation in uniaxial compressive strength values (MPa) of the samples in dry and wet state (dry and wet states are shown by blue and pink lines, respectively).

2.3.3 Durability Features

The durability features of the samples were estimated by using the Winkler’s equation (1986), which had been originally developed for the durability estimation of rocks.

$$D = (UCS_{wet} / UCS_{dry}) \times 100$$

where, D: durability

UCS_{wet}: uniaxial compressive strength of material in wet state

UCS_{dry}: uniaxial compressive strength of material in dry state

The durability classification based on the results of this equation is as follows:

Excellent durability → D is in between 100 and 80

Good durability → D is in between 80 and 70

Fair durability → D is in between 70 and 60

Poor durability → D is in between 60 and 50

The results are shown in Table 7 and Figure 8.

Table 7 Durability features of the samples

Bricks	UCS (MPa)		D(index)	D(class)
	DRY	WET		
Reddish brown				
TB 1	5.8	4.3	74.1	Good
TB 3	9.4	4.7	50.1	Poor
TB 4	5.2	3.2	61.7	Fair
TB 5	4.0	3.2	78.8	Good
TB 6	6.3	3.2	50.2	Poor
TB 7	4.6	4.0	88.0	Excellent
TB 8	5.4	5.2	95.4	Excellent
TB 9	7.4	6.7	90.8	Excellent
Pale brown				
TB 12	8.4	5.6	66.4	Fair
TB 13	7.1	5.5	77.9	Good
TB 16	5.7	3.6	64.3	Fair
TB 17	12.3	8.3	67.4	Fair
TB 18	7.5	6.2	82.3	Excellent
TB 19	5.2	3.1	60.6	Fair
Brown				
TB 20	10.4	7.0	67.7	Fair
TB 21	12.6	9.3	73.9	Good
TB 22	13.8	11.7	85.0	Excellent
Dull brown				
TB 24	9.8	9.6	97.3	Excellent
Mortars				
TM 1	7.3	5.6	77.7	Good
TM 2	2.9	2.5	84.0	Excellent

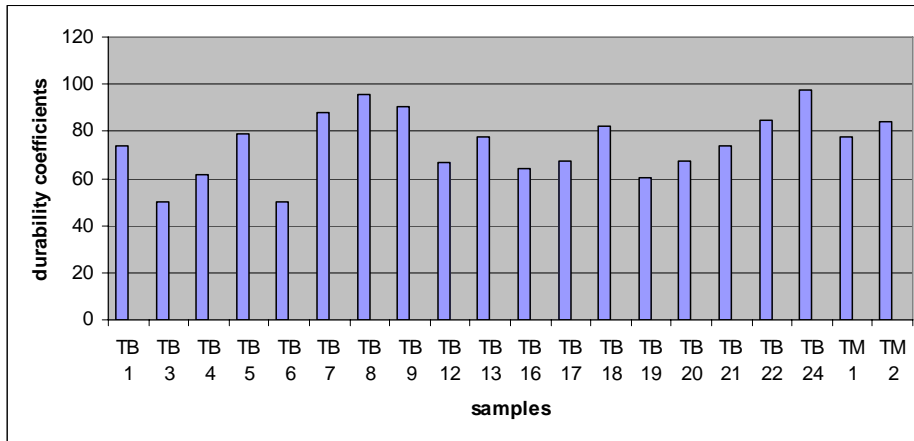


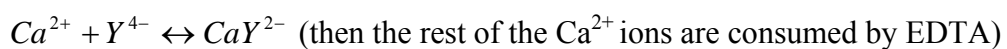
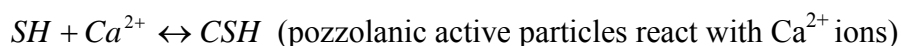
Figure 8 Variation in durability features of the samples

2.4 Pozzolanic Activity Measurements by EDTA Titration

Pozzolanic materials are those, which do not react directly with water, but react with lime in the presence of water and form water-insoluble compounds having binding properties. The capacity of those materials to react with lime is expressed as pozzolanic activity. Thus, a material having higher pozzolanicity is expected to produce more water insoluble compounds such as various calcium silicate hydrates (CSH), which contribute to the strength of final product.

There are two frequently used methods to measure the pozzolanic activity, which are (1) electrical conductivity, and (2) EDTA titration. The former method is based on the measurement of the change in electrical conductivity. In this study, the latter method was utilized and then the results were expressed in terms of change in electrical conductivity.

Pozzolanic activity of bricks and fine aggregates of mortars were determined as follows: Brick samples were crushed into fine grains in an agate mortar. The mortar samples were dissolved in 5% hydrochloric acid to get rid of the acid soluble binder part, as carbonated lime (CaCO_3) and calcium silicate hydrates (CSH). Unfortunately, acid soluble aggregates, such as limestone, also dissolve during that treatment. Remaining insoluble part was filtered and washed away from hydrochloric acid. For the purpose of checking that all acid was washed away, the spot test for Cl^- ions was carried out, i.e. several drops of test solution was taken into a tube and treated with several drops of dilute nitric acid (2N, HNO_3) and silver nitrate solution (0.1 N AgNO_3). It was controlled if a “whitish-blue gelatinous” precipitation formed or not whose formation showing the presence of chloride ions (Teutonico, 1988; 63). After being sure that insoluble part was totally free of hydrochloric acid, mortar aggregates were dried. Mortar aggregates and brick samples were sieved. The particles smaller than 125μ in size were separated by means of a standard sieve set. 0.05 g of each sample under 125μ size were put into the containers having 30 ml of Ca(OH)_2 saturated aqueous solution and covered tightly. A container having saturated Ca(OH)_2 solution without any brick or mortar aggregate sample was used as standard. The samples were left in the containers for two weeks. After this period 10 ml of each solution was titrated with 0.01 M EDTA (Ethylenediamine tetra-acetic acid) standard solution using an indicator (calgon). pH of the solution was kept at 12-13 using 10% NaOH solution. Since pozzolanic active particles react with Ca^{2+} ion, and EDTA consumes the rest of Ca^{2+} ions, the differences between the sample solutions and standard Ca(OH)_2 solution gives a value for pozzolanicity of brick and mortar aggregates. The reactions taking place are as follows:



The results were expressed in terms of the drop in electrical conductivity (ΔEC) as 25 g of aggregate kept in 1 lt of $Ca(OH)_2$ saturated solution (Luxan *et al.*, 1989; TS EN 196-5, 2002).

The results are shown in Table 8 and Figure 9.

Table 8 Pozzolanic activity values (ΔEC) of the samples

	Consumed EDTA(ml)	ΔEC mS/cm
STANDARD	24.0	0.0
Bricks		
Reddish brown		
TB 2	22.0	6.0
TB 10	20.5	10.5
TB 11	24.1	0.0
Pale brown		
TB 13	21.0	9.0
TB 14	22.4	4.8
Brown		
TB 20	21.1	8.7
TB 21	20.0	12.0
Dull brown		
TB 24	16.8	21.6
Mortars		
TM 1	23.5	7.5
TM 2	21.5	18.0

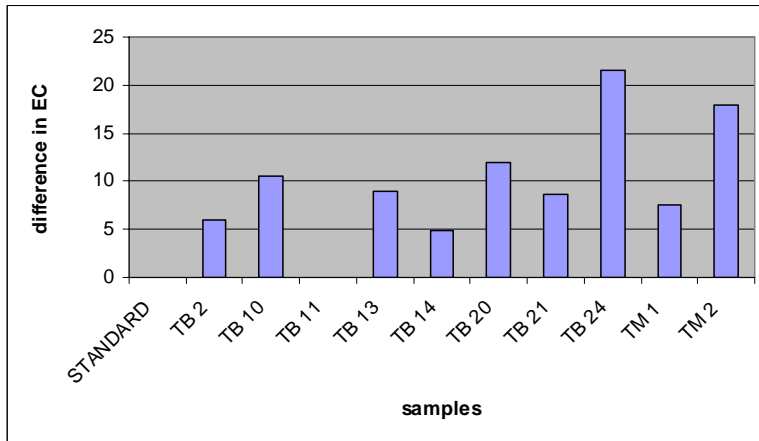


Figure 9 Variation in pozzolanic activity values (ΔEC) of the samples

2.5 Discussion of Results

In this section, results of the laboratory analyses related with the basic physical and mechanical properties of the samples as well as their durability and pozzolanic activity features were discussed. The average values for each group of samples are indicated in Table 9 and Table 10.

Table 9 Resultant average values for physical properties (effective porosity, bulk density and water absorption capacity WAC) and modulus of elasticity (as average \pm standard deviation)

Type of Samples	Number of Samples	Effective Porosity (%)	Bulk Density (g/cm ³)	WAC (%)	E _{mod,dry} (MPa)	E _{mod,wet} (MPa)
Bricks	24					
Reddish brown	11	50 \pm 1	1.35 \pm 0.03	37 \pm 2	985 \pm 188	801 \pm 204
Pale brown	8	51 \pm 1	1.36 \pm 0.04	38 \pm 2	1165 \pm 216	869 \pm 184
Brown	4	44 \pm 2	1.49 \pm 0.02	30 \pm 1	1249 \pm 263	756 \pm 493
Dull brown	1	32	1.78	18	1440	1408
Mortars	2	40 \pm 1	1.53 \pm 1.50	26 \pm 2	684 \pm 227	456 \pm 229

The results obtained in this study appeared to be comparable to those reported as a result of the laboratory analyses carried by Tuncoku (1993 and 2001) for many Seljuk period structures including Tahir ile Zühre Mescidi, the subject of this thesis.

Physical properties determined in this study are effective porosity, bulk density, water absorption capacity (WAC). *Effective porosity* values change between approximately 32 % and 53 % for the majority of the samples tested (Table 2 and Figure 2). Moreover, the values are close to each other for brick and mortar. This is valid also for the resulting *bulk density* values, that are in the range of 1.31 and 1.57 g/cm³ for most of the samples (Table 3 and Figure 3). As seen, the range is rather narrow, indicating a rather uniform distribution of the materials' properties within the structure in terms of those characteristics. That compatibility feature between original construction materials surely contributes for brick and mortar to work together under related physical phenomena. As expected, the samples with lower bulk density have higher porosity. As average values, reddish brown and pale

brown samples are more porous than the other ones. The dull brown sample (TB 24), on the other hand, appears to be less porous and therefore more dense.

For the same samples, the *water absorption capacity* change within the range of 18-40 % (Table 4 and Figure 4). In this case, the samples with higher porosity have higher water absorption capacity, since those two characteristics are interrelated. Therefore, TB 24 is the sample having the lowest water absorption capacity, while reddish brown and pale brown brick samples have the highest.

Mortar samples are less porous and denser than the major part of brick samples, however the difference is not at all considerable. Therefore, the compatibility between brick and mortar materials in terms of physical features can be concluded.

In this study, the *modulus of elasticity* values were determined by ultrasonic velocity testing. It was observed that, moduli of elasticity of tested bricks appeared to change within the range of 1878 MPa-554 MPa and those of mortars within 457 MPa-1124 MPa (Table 5 and Figure 5). These values are comparable with those found by Tuncoku (2001) at his study carried out for a series of Seljuk period structures, and the values reported here can be positioned close to the lower bound of the interval reported by him. However, the values are much lower than the Young's Modulus values of Hagia Sophia bricks, which are in the order of 3100 MPa as estimated by Çakmak *et al.* in 1995. On the other hand, the moduli of elasticity values determined by Çakmak *et al.* (1995) for the mortars of Hagia Sophia fall within the range of the results obtained in this study. The modulus of elasticity values obtained for the Byzantine monuments in Kiev (Moropoulou *et al.*, 2000: 606) are also consistent with the results obtained here. At the latter, the moduli of elasticity were estimated for the bricks and mortars, as 1000-3000 MPa and 600-700 MPa, respectively. In that study, the Young's Modulus of brick and mortar composite were given as 2200 and 2500 MPa for Hagia Sophia (Moropoulou *et al.*, 2002: 544).

Table 10 Resultant average values for uniaxial compressive strength (UCS), pozzolanicity and durability (D) (as average \pm standard deviation)

Type of Samples	Number of Samples	UCSdry (MPa)	UCSwet (MPa)	Pozzolanic Activity (Δ EC)	D(index)	D(class)
Bricks	24					
Reddish brown	11	6.0 \pm 1.3	4.3 \pm 0.9	5.5 \pm 3.7	73.6 \pm 14.7	Good
Pale brown	8	7.7 \pm 1.8	5.4 \pm 1.3	6.9 \pm 2.1	69.8 \pm 6.9	Fair
Brown	4	12.2 \pm 1.2	9.3 \pm 1.6	10.4 \pm 1.7	75.5 \pm 6.3	Good
Dull brown	2	9.8	9.6	21.6	97.3	Excellent
Mortars	1	5.1 \pm 2.2	4.1 \pm 1.6	12.8 \pm 5.3	80.9 \pm 3.2	Excellent

In this study, the resulting modulus of elasticity and uniaxial compressive strength values of a previous study (Tuncoku, 2001) carried out for the mortars of a series of Seljuk period structure were utilized for developing a second degree relation between those characteristics (Figure 6). Therefore, *uniaxial compressive strength* values for the samples studied here were derived inserting the modulus of elasticity results into that equation. The uniaxial compressive strength values obtained in this way are consistent for mortar samples with the values proposed at the literature and with the results of Tuncoku. Accordingly, the uniaxial compressive strengths of mortars are in between 2.9 MPa and 7.3 MPa in dry state, and 2.5 MPa and 5.6 MPa in wet state (Table 6 and Figure 7). The obtained ranges for the bricks are 5.2 MPa-13.8 MPa and 3.1 MPa-11.7 MPa for dry and wet states, respectively. The uniaxial compressive strengths of bricks appeared to be rather low in comparison with the values available in the related literature. That can be due to that the correlation between modulus of elasticity and uniaxial compressive strength was developed taking into consideration the data set obtained from mortars, and that was used for bricks as well. Because of these assumptions made during the calculations, the

reported uniaxial compressive strength values should be accepted as average values. Reddish brown bricks are the ones with lower uniaxial compressive strengths in comparison with the other sets, determined according to their colours. The average value of that group, which was very low (6.4 MPa) was not reasonable for historic bricks. On the other hand, it was seen that the brown sample set had generally higher uniaxial compressive strength values, among which TB 22 had the highest in both dry and saturated states. The average value for that group was normal for historic bricks and consistent with the results of other studies. The uniaxial compressive strength of TM 1 was within the range of uniaxial compressive strengths of bricks, however, that of TM 2 was relatively low.

According to the classification that Luxan made (Luxan *et al.*, 1989), a ΔEC value higher than 1.2 mS/cm can be accepted as good *pozzolanic activity*. Therefore, all the samples that were studied here have good pozzolanic activity features, except one sample, TB 11, which appeared to have no pozzolanicity (Table 8 and Figure 9). The most pozzolanic sample was TB 24, whose different appearance and characteristics were mentioned before. Tuncoku (2001), using only electrical conductivity method, had concluded that most samples appeared to have good pozzolanic properties too.

Durability features were determined according to the equation proposed by Winkler, based on the uniaxial compressive strength information in dry and wet states. According to that equation given in 2.3.3, the rate of change of uniaxial compressive strength values in dry and wet state gave an index of durability, i.e. the lower the uniaxial compressive strength in wet state than that in dry state, the less durable the material was, and vice versa. It can be concluded that (Table 7 and Figure 8) majority of the samples studied here appeared to have good to excellent durability, as the standing historic structure for more than eight centuries proved that itself.

As a general conclusion, the results obtained by the laboratory studies carried out within this study are parallel with the results found at the mentioned previous studies. Therefore, those values can be accepted as the characteristic values for Seljuk period brick and mortar construction materials. However it should be noted that in this study, the analysis of several parameters involved a lot of approximations. First of all, the values obtained by means of ultrasonic velocity measurements may include experimental errors. Moreover, it is not fully known whether the wet modulus of elasticity values reflect correctly the strength properties or not. Therefore, their usage in the equation of uniaxial compressive strength as a function of modulus of elasticity, obtained by utilizing a data set from a previous study to reach to the wet uniaxial compressive strengths, is an approximation too. Another point that should be taken into account is that the data set utilized for the derivation of this formula included the uniaxial compressive strength values converted from point load test values. Uniaxial compressive strength values obtained from point load test results, however, may not reflect the actual uniaxial compressive strength of material.

2.6 Tensile Strength Value

Tensile strength determination had not been carried out neither by Tuncoku (2001) and nor by this study. As mentioned in Chapter 1, the tensile strength of masonry is very low and it can be accepted as even zero for the sake of simplicity. However, the literature survey revealed some studies including tensile strength determination as well. By Moropoulou *et al.* (2002) a tensile strength for mortars was assumed around 1 MPa - 2 MPa, within the framework of a study on Hagia Sophia (Moropoulou *et al.*, 2002: 543). The same authors found out that the tensile strength of a typical mortar-brick sandwich sample was 0.4 MPa - 0.5 MPa. The same experiment repeated in another laboratory gave the value of 0.5 MPa - 1.2 MPa for

the same aim; two-split cylinder test, on the other hand, gave a narrower band result of 0.7 MPa - 1.2 MPa.

CHAPTER 3

STRUCTURAL INVESTIGATION

3.1 Physical Description of the Upper Structure of Tahir ile Zühre Mescidi

Tahir ile Zühre Mescidi, which is located at Beyhekim District in Konya, is composed of a prayer hall, a türbe (tomb) and an entrance hall providing access from outside to prayer hall. Türbe cannot be passed from either prayer hall or entrance hall; and the door from outside is closed with bricks. The prayer hall and turbe have squared plans and are covered with domes, while the entrance hall is covered with a vault. The construction materials used are stone from the foundation up to some height of the walls, and brick for the rest of the walls and for the superstructure. Glazed ceramic tiles and gypsum renderings can be seen for decoration purposes. Detailed information on the physical description of Tahir ile Zühre Mescidi can be found in the studies made by Tuncoku (1993) and Katoğlu (1966).

In terms of structural behaviour, this study dealt fundamentally with the dome of prayer hall and the Turkish triangles providing the transition from circular dome plan to square-shaped inner space plan type. The dome is approximately 6.0 m and 6.65 m in internal and external diameter, respectively, and is semispherical. The dome is placed upon a sixteen-sided tambour. This tambour is 0.3 m high and is supported by Turkish triangles, which provide the transition from a circular plan to a square one. This transition is provided within a height of 1.45 m.

The dome part of the masjid has a zigzag pattern formed by vertical-horizontal (orthogonal) stack of bricks. The pattern is repeated from dome centre to dome tambour, extending in size (Bakırer, 1972: 193). At the vault, cut bricks have been used. (Bakırer, 1972: 198). Bricks that were used for the construction of the superstructure of Tahir ile Zühre Mescidi are whole (21.5 x 21.5 x 4 cm.), half (11 x 21.5 x 4 cm.) and quarter bricks (4 x 4 x 4 cm.) (Tuncoku, 1993: 26). However, at the main dome, the dimensions of bricks are 9 x 19 x 6 cm. The thicknesses of mortar bed joints are 3 cm, whereas those of rising joints are 2 cm (Bakırer, 1981: 469-472).

Tuncoku (1993) described the state of the dome. There were few minor cracks at the east and west of the dome, internally, caused by water penetration. There were some losses in bricks and mortars, however, the dome has no any important structural problems that could be seen visually (Tuncoku, 1993: 30).



Figura 10 Dome of Tahir ile Zühre Mescidi

3.2 Safety of a Structure

Safety of a structure is defined as the reserved resistance of the structure to collapse and it is reflected to the structure to eliminate the uncertainties at its design arising from the assumed loading conditions, to the material properties and during construction phase. Safety is measured by the safety coefficient (margin on safety), which is theoretically equal to the ratio of the resistance of structural element to the loads that is subjected to, in other words, to the ratio of ultimate failure load to allowable load. The exact determination of such a ratio requires a detailed analysis of geometrical form, loads and loading conditions, soil, and foundation, which is very difficult. Therefore, it is not possible to give a definite numerical value (Heyman, 1982: 9, 36).

3.3 Dome as a Structural Form

“Nearly all masonry spanning elements” (including not only arches, domes and vaults but also architraves and lintels) have rather large margin of safety (Mainstone, 1989: 71). This is firstly due to the stable geometry of arch like structural elements (Heyman, 1982: 10). Another factor providing this high margin of safety is the over design of sectional dimensions, which is generally the case with historic structures. The thickness of ring should be large enough to provide that the thrust line developing from the applied loads lies totally within the section (O’Dwyer, 1999: 187). The line of thrust is a theoretical line equal to the funicular polygon, and is defined as the line containing all the points where the stress resultants act at every section of the arch. It gives idea about the possible failure mechanisms as well, showing the points where the line of thrust is close to the

boundary of section and those where the thrust line touches to the boundary, which leads to the formation of a hinge point. In addition to these factors, material properties, as mentioned before, play an important role on the stability of any structural element. In the case that material properties are not mechanically sufficient to resist the loading conditions that the structure is subjected to, the formation of structural defects is inevitable. Similarly, the physical characteristics of the materials should be sufficient enough to face the environmental conditions at the zone in which the structure is situated.

A dome can be defined as a three-dimensional arch system. It exhibits a shell behaviour, which means the capability of the structural element to carry the applied loads within one or two-curvature planes. Shell can be modelled as a curved surface, whose thickness is relatively small in comparison with the dimensions of the structure (Heyman, 1995: 28).

3.4 Derivation of Mechanical Data to be Used in Structural Analyses

By the laboratory analyses, the uniaxial compressive strength values of brick and mortar were determined separately. For the structural analysis part of the study, however, a composite value for the masonry was needed. There are several standards to calculate this integrated value. In this study, TS ENV 1996-1-1 (EUROCODE 6) was taken as reference.

According to the mentioned code, the compressive strength of masonry was calculated as follows:

$$f_k = K f_b^{0.65} f_m^{0.25}$$

where, f_k : strength of masonry

f_b : strength of brick

f_m : strength of mortar

K: constant

As can be seen at the results of the previous chapter, it was seen that the obtained uniaxial compressive strengths were very low in comparison to the relevant literature. Only the values determined for brown sample set were reasonable. Therefore, for the modelling part of this study, f_b was accepted to be 12 MPa. f_m , on the other hand, was taken as 4.5 MPa, which was the obtained average and a normal value for historic mortars. According to the written criteria at the standard, K was taken as 0.60. Therefore, f_k was calculated as 4.4 MPa.

For a composite strength value of masonry in wet state, f_b and f_m were accepted to be 9 MPa and 3 MPa, respectively. As a result, $f_{k,wet}$ was found as 3.3 MPa.

In this study, tensile strength of masonry was taken as 1/10 of the compressive strength value. Therefore, in dry state, tensile strength value was taken as 0.4 MPa, which is also a reasonable value reported in literature (Moropoulou *et al.*, 2002: 543). Tensile strength in wet state was taken as 0.3 MPa, again as 1/10 of the compressive strength value of masonry in wet state.

For defining composite value of modulus of elasticity, compatibility of deformation principle was utilized. According to Hooke's Law, deformation can be represented in terms of loading, geometry and material property as follows:

$$\delta = \frac{PL}{AE}$$

where, δ : axial deformation

P: internal load at section

L: section length

A: section area

E: modulus of elasticity of section material

Let's think of a layer brick and a layer mortar, one on the other. A load, P, is applied in perpendicular manner to their plane. In this case, L's are the thickness of brick and mortar. The total deformation of unit masonry layer, composed of a brick layer and a mortar layer, one on the other, should be equal to the sum of the deformations of brick and mortar layers.

$$\delta_{total} = \delta_{brick} + \delta_{mortar}$$

where, δ_{total} : total deformation of brick and mortar layers

δ_{brick} : deformation of brick layer

δ_{mortar} : deformation of mortar layer

$$\frac{Pt_{total}}{AE_e} = \frac{Pt_{brick}}{AE_{brick}} + \frac{Pt_{mortar}}{AE_{mortar}}$$

where, t_{total} : total thickness of brick and mortar layers

t_{brick} : thickness of brick layer

t_{mortar} : thickness of mortar layer

E_{brick} : modulus of elasticity of brick

E_{mortar} : modulus of elasticity of mortar

E_e : effective modulus of elasticity of masonry

Since the applied loads, P, and the section areas, A, are the same for both layers, the formula became:

$$\frac{t_{brick} + t_{mortar}}{E_e} = \frac{t_{brick}}{E_{brick}} + \frac{t_{mortar}}{E_{mortar}}$$

At Tahir ile Zühre Mescidi, $t_{brick} = 9$ cm, and $t_{mortar} = 3$ cm. E_{brick} and E_{mortar} were taken 1100 MPa, and 800 MPa as average values. By using the above formula, E_e was found approximately as 1005 MPa.

To determine the composite value for wet modulus of elasticity, E_{brick} and E_{mortar} were taken as 900 and 650 MPa, respectively, and $E_{e,wet}$ was found as 821 MPa.

Shear strength of the material was calculated according to the formula given below:

$$\tau = \tau_0 + \mu * f_n$$

where, τ : shear strength (MPa)

τ_0 : cohesion (taken as 0.2, as suggested by Ünay, 2002)

μ : internal friction angle (taken as 0.2, as suggested by Ünay, 2002)

f_n : compressive strength (MPa)

Therefore, $\tau = 0.2 + 0.2 \times 4.4 = 1.08$ MPa.

In the wet state, $\tau = 0.2 + 0.2 \times 3.3 = 0.86$ MPa.

3.5 Dome Behaviour in General

To understand the behaviour of the dome under its self-load, this simplified two dimensional semicircular arch example seen in Figure 11 can be utilized.

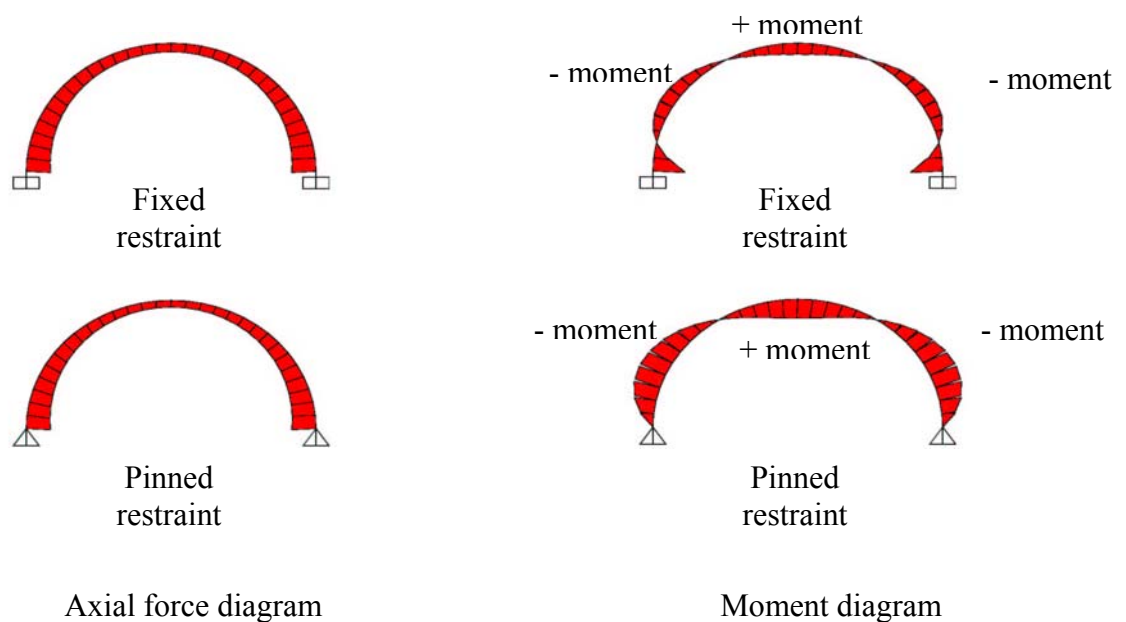


Figure 11 Axial stress and moment diagrams of semicircular arches in pinned and fixed restraint conditions, above and below, respectively.

The arches shown in figure 11 are under their self-loads and the change of axial stresses and moments in this case are seen. The stresses developing at the inner and outer surfaces of a structure are a combination of the stresses due to axial load and those due to moment (Figure 12). In the structure analysed here, the restraint condition should be in between these two examples, i.e. it is neither the fixed end,

which does not allow any movement, nor the pinned end, which allows rotation. The rigidity and geometry of Turkish triangles determine the restraint condition. In this study, the restraint conditions were accepted to be fixed, taking into account the shape of the squinches, wall thickness, weight of the superstructure, and substructure rigidity.

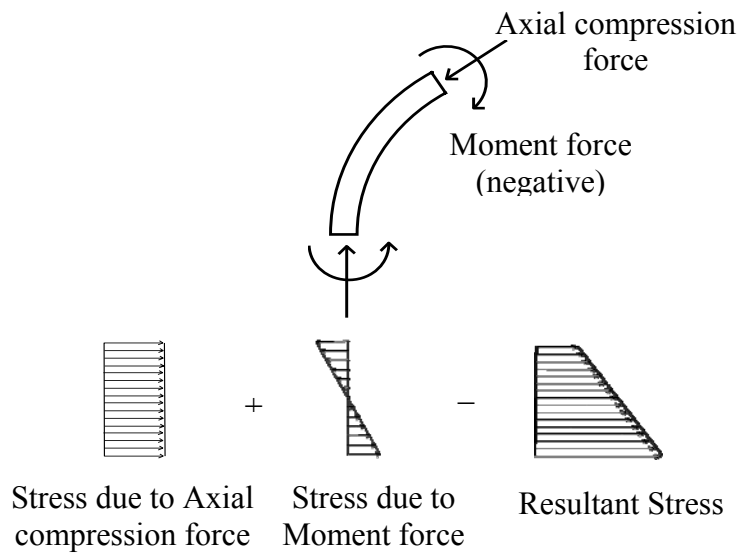


Figure 12 Resultant stress due to axial and moment forces

Figure 13 shows the local axes' sign convention followed all throughout this study.

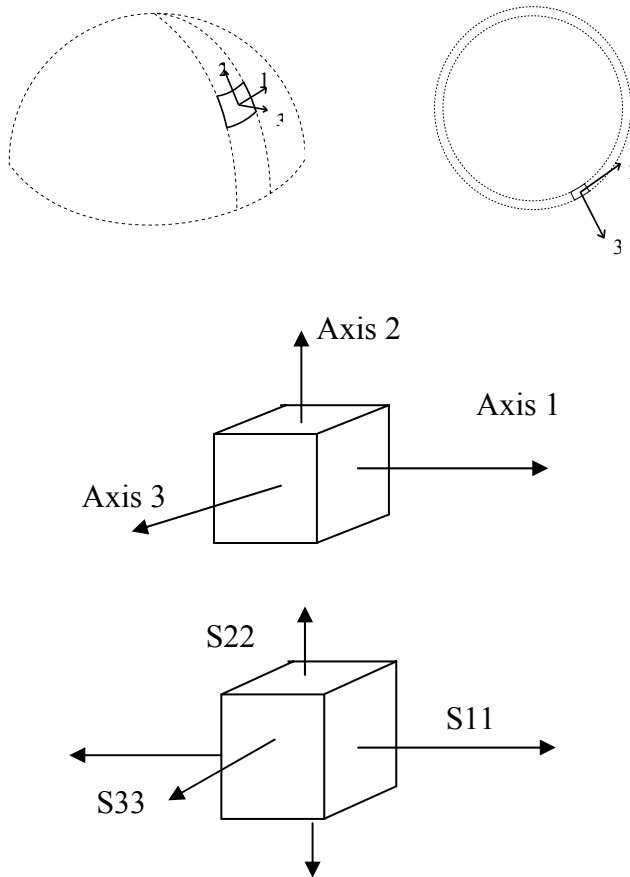


Figure 13 Local axes directions and corresponding stress directions used in this study

3.6 Computer Modelling of the Upper Structure of Tahir ile Zühre Mescidi

For the structural analysis of the upper structure of the masjid, a computer model was constructed, in accordance with its actual geometry. For each analysis that was carried out in this study, a shell model composed of 2448 areas was used (Figure 14). The obtained material properties were inserted into the program, SAP 2000. Firstly, five different load cases, which represent the normal service conditions, were assigned: (1) self-load, (2) wind load, (3) snow load, (4) temperature load and (5) earthquake load and the effect of their appropriate combinations were tried to be

simulated. Then, the temperature induced forces and strains at the interface were studied in the cases of (6) the partial collapse of the superstructure which is then completed with cement and (7) a concrete coating layer over the superstructure.

Since this was not a design, but the analysis of an existing structure, neither design factors nor safety coefficients were used. Similarly, common load combination coefficients were not used either. The results were represented as graphic output. According to this, each colour corresponds to a stress interval, which is represented at the bottom. Positive values means tensile stress formation, while negative ones are compression. All stress values were reported in MPa.

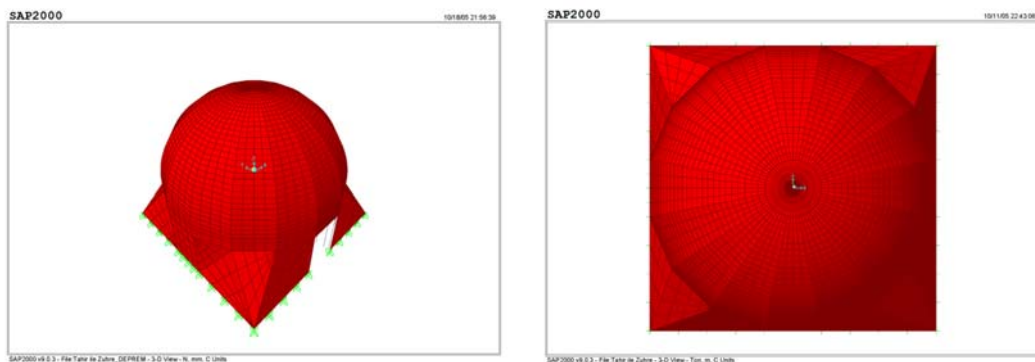


Figure 14 3D view and top view of the model of the upper structure of Tahir ile Zühre Mescidi

3.6.1 Structural Behaviour of the Upper Structure under Dead Load

The structural analyses' part of the study was started with the analysis of the superstructure under dead load. Dead load was calculated by the software itself using the material density and geometry information.

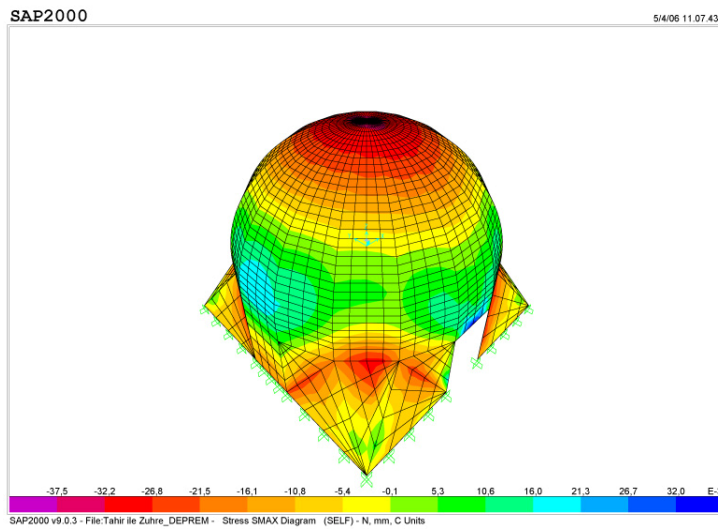


Figure 15 3D view of SMAX diagram of the upper structure of the monument under dead load

Figure 15 shows the maximum tensile stress distribution of the superstructure under its dead load. As the figure indicates, the structure exhibits typical dome behaviour under vertical loading, i.e. it tries to shrink at top and bottom since the base conditions does not allow lateral movement. The middle part, on the other hand, tends to widen out. Therefore, at the top and bottom compression stresses develop,

whereas tension forms in the middle part.

The developing stresses are in the order of 0.030 MPa in compression and in tension. These are the values far less than 4.4 MPa and 0.4 MPa, the compressive and tensile strength of the material, respectively.

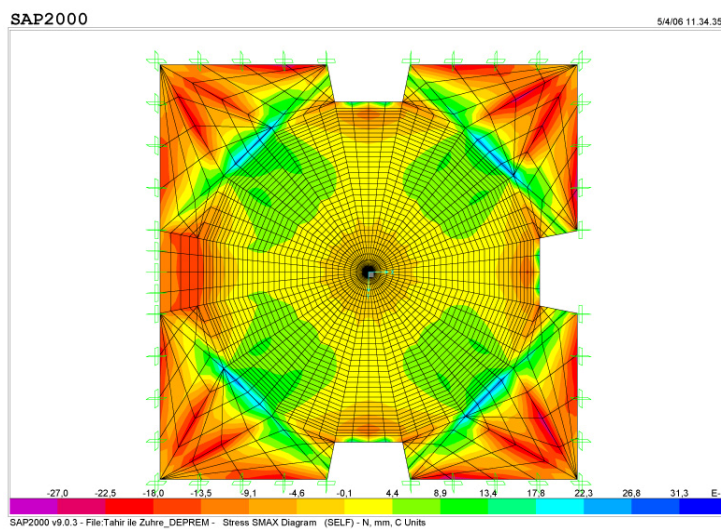


Figure 16 Bottom view of SMAX diagram of the upper structure of the monument under dead load

Figure 16 shows the inner surface of the dome. The structure tends to bend to inside under its self-load. Therefore, tensile stress forms at the outer surface, whereas at the inner surface compression develops. Table 11 gives the resulting base reactions under this loading condition.

Table 11 Base reactions under self load

OutputCase	GlobalFX (N)	GlobalFY (N)	GlobalFZ (N)
SELF	2,012E-07	0,00000025	721741,62

As seen the base reaction values appeared to be very low. Having controlled the resulting base reactions under self load as well, it can be concluded that the structure is safe under its self-load.

3.6.2 Structural Behaviour of the Upper Structure under a Combination of Dead Load, Snow Load and Wind Loads

As a possible service condition during winter, the structural behaviour of the upper part under a combination of its self-load, snow load and wind load was investigated. To define the wind load, TS 498 was utilized. For a structure, whose height is less than 8 m, the wind velocity defined by the standard is 28 m/s and the corresponding load is 50 kg/m². Snow load was taken as 75 kg/m² for Konya, according to TS 498. Both loads were applied in projected gravity direction, i.e. downwards and in a way that it's quantity changes according to slope of the structure. Therefore, at the top of the dome, wind and snow load apply in defined quantity and towards the slope of the dome it decreases to cosine of the load as to become zero at the edges.

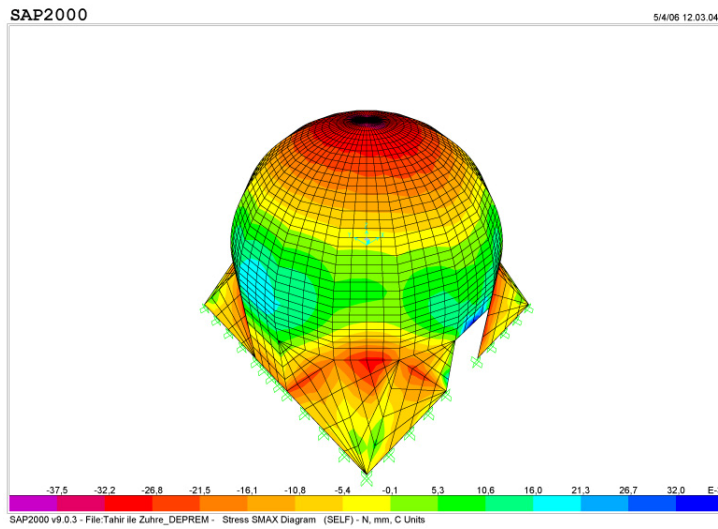


Figure 17 3D SMAX diagram of the upper structure of the monument under the combination of its dead load, snow load and wind load

As seen, Figure 17 is very similar to the SMAX diagram of the structure under only self-load, in terms of developing stresses. That means the effects of snow and wind loads are very small. This can be seen from the resulting base reaction values as well (Table 12). Even in the case that whole structure is accepted to be wet and the $f_{k,wet}$ value (3.3 MPa) is used in the evaluation of the resulting stress values, the structure was appeared to be safe under the mentioned load combination.

Table 12 Base reactions under self load, snow load and wind load

OutputCase	GlobalFX (N)	GlobalFY (N)	GlobalFZ (N)
SELF	2,012E-07	0,00000025	721741,62
SL	1,003E-08	1,24E-08	21014,68
WLX	-10957,31	-1,646E-09	-3,623E-08
SELF+SL+WL	-10957,31	2,607E-07	742756,3

The effects of wind and snow load were tried to be seen separately as well (Figure 18 and Figure 19).

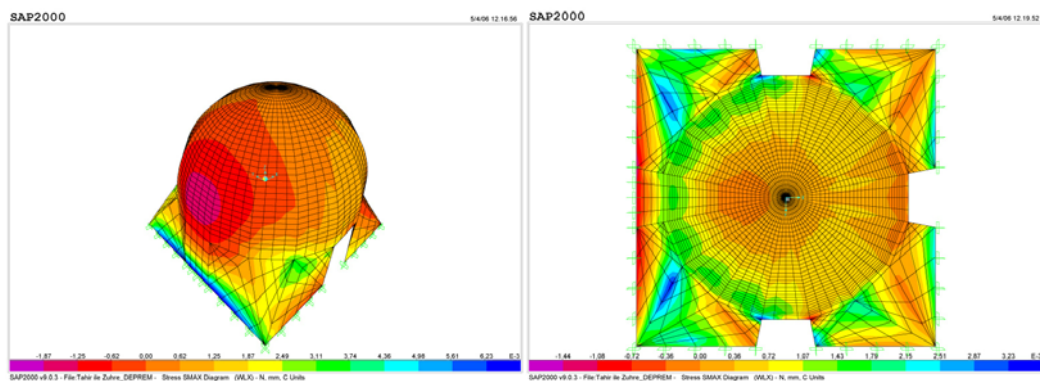


Figure 18 3D deformed and bottom view SMAX diagram of the upper structure of the monument under wind load

The wind load was applied in the positive x direction. Because of this reason, at the outer surface compression forms in the positive x direction and tension at the opposite side as can be comprehend from the deformed shape as well. The stresses were in the range of 0.0016 MPa in compression and 0.0072 MPa in tension.

Therefore, the resulting stresses due to wind load were insignificant in comparison to the compressive and tensile strengths of the material. The effect of snow load was expected again not to be big.

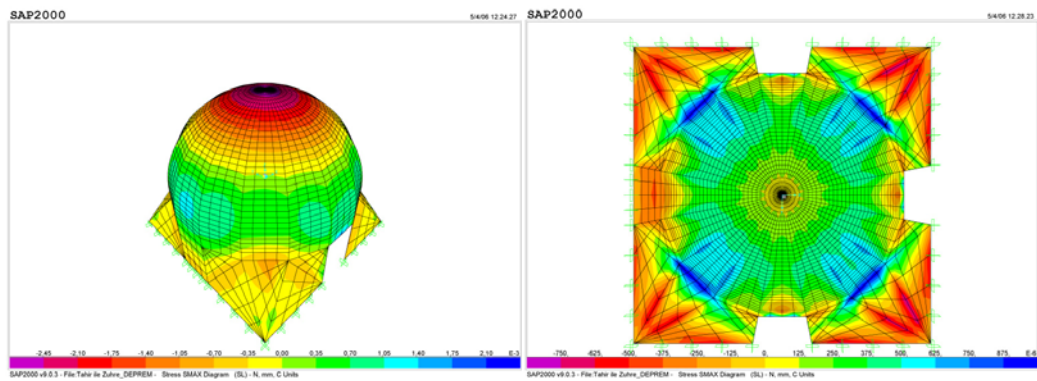


Figure 19 3D and bottom views SMAX diagram of the upper structure of the monument under snow load

As expected, the resulting stresses were in the order of 0.0007 MPa in compression and 0.001 MPa for tension, which are even smaller than those resulted under wind load.

As a result, the structure has a big safety margin under a combination of self-load, wind load and snow load.

3.6.3 Structural Behaviour of the Upper Structure under Temperature Load

In this part, the effect of a partially applied temperature load due to a temperature difference of 25°C was investigated to simulate the effect of an eventual sun exposure. The area to which the temperature difference applied for this purpose was shown in Figure 20.

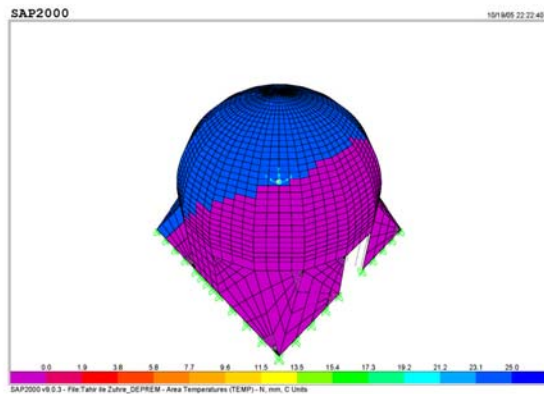


Figure 20 Applied temperature load of 25°C. Dark blue indicates the part warmer.

For the purpose of reflecting the normal conditions in a more realistic manner, the effect of dead load was not excluded. Figure 21 shows the resulting SMAX diagram in the case of a combination of dead load and the mentioned temperature load.

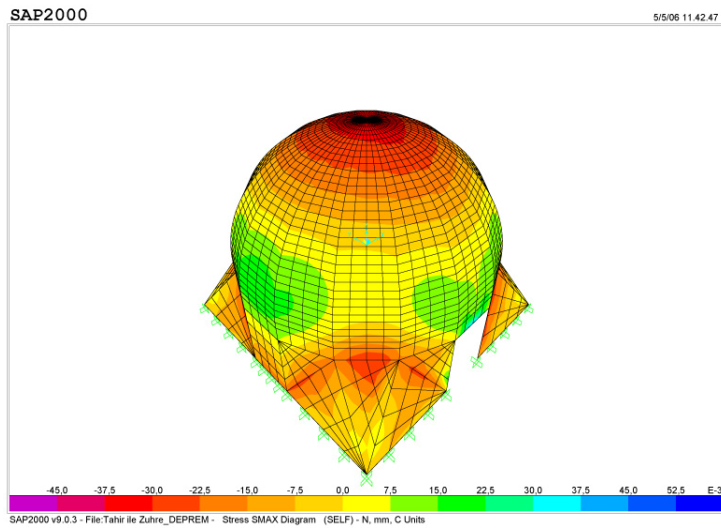


Figure 21 3D SMAX diagram of the upper structure of the monument under the combination of dead load and temperature load

As seen from Figure 21 which is, again, very similar to SMAX diagram of the upper structure under dead load only, it was understood that the effect of dead load is bigger than the assigned temperature load, as expected. Figure 22 shows the effect of temperature load alone.

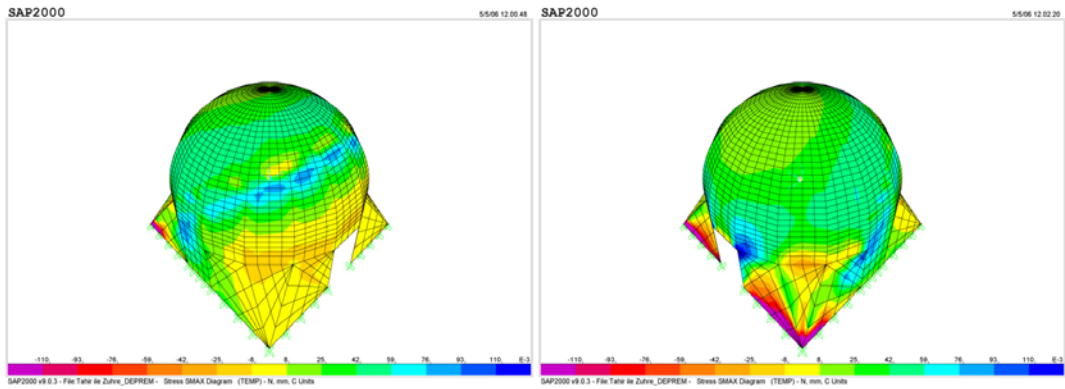


Figure 22 3D SMAX diagrams of the upper structure of the monument under temperature load

Since the temperature load was defined as a positive temperature difference, the structure tries to expand at its warmer part. This situation results in tensile stress formation at the outer part of the dome.

The developing stresses are again very low, being in the range of 0.1 MPa for tension is 0.2 MPa for compression which are smaller than the compressive and tensile strength of the material, 0.4 MPa and 4.4 MPa, respectively.

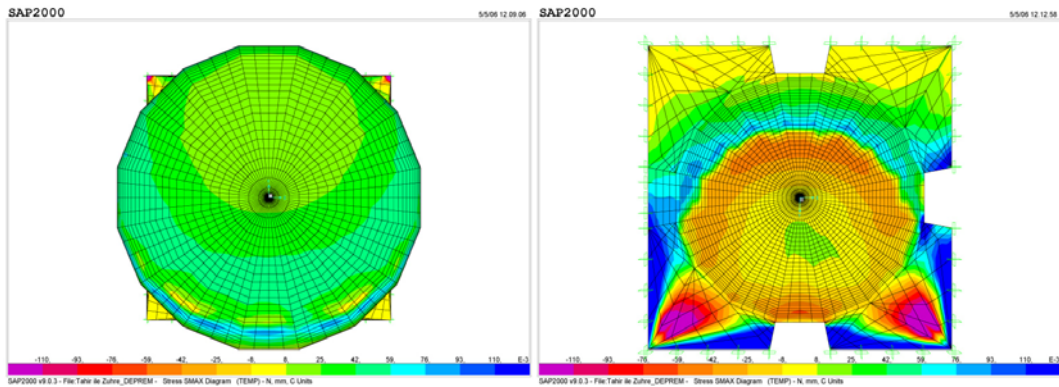


Figure 23 Top and bottom views of SMAX diagram of the upper structure of the monument under temperature load

Table 13 Base reactions under temperature load and dead load

OutputCase	GlobalFX (N)	GlobalFY (N)	GlobalFZ (N)
TEMP	-5,123E-07	-6,293E-07	-0,00004258

As can be seen from Table 13, the resulting base reactions under temperature load are very low, as expected.

3.6.4 Structural Behaviour of the Upper Structure under Earthquake Load

For historic structures, which stand for centuries under their self-loads and the loads arising from environmental conditions, earthquake is generally the governing factor. For this reason in this study, earthquake analysis was carried out as well.

According to TS 498 (Turkish Standards), Konya is located at the 4th earthquake region. The corresponding effective ground acceleration coefficient should be 0.1, which means that the acceleration affecting the structure will be 0.1 times g, gravitational acceleration, which is equal to 9.81 m/s².

Since in this study, the whole structure was not modelled, it was assumed that the modelled part sits on soil. The soil information was unknown, therefore to be on the safe side, it was assumed to be Z4, the worst soil type. The response spectrum shown below is a graphic representation of the ratio of the maximum acceleration, which the structure is subjected to, normalized with the gravitational acceleration versus different natural frequencies for the assumed soil type.

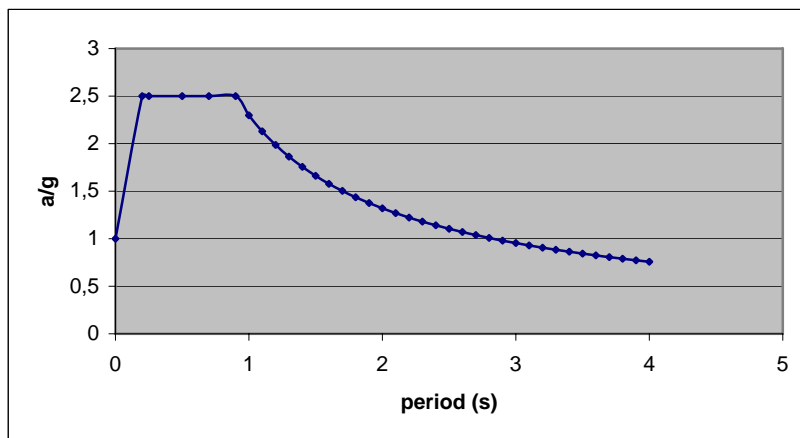


Figure 24 Response spectrum according to ABYYHY 98 (Turkish Earthquake Resistant Design Code 1998) for the soil type Z4

The earthquake load was applied in both x and y directions, and a response spectrum analysis was carried out, which shows the maximum response of the structure to earthquake. Figure 25 shows the deformed shape under the mentioned loading condition, while Figure 26 and Figure 27 show the S11 and S22 distributions, respectively (for sign convention, see Figure 12).

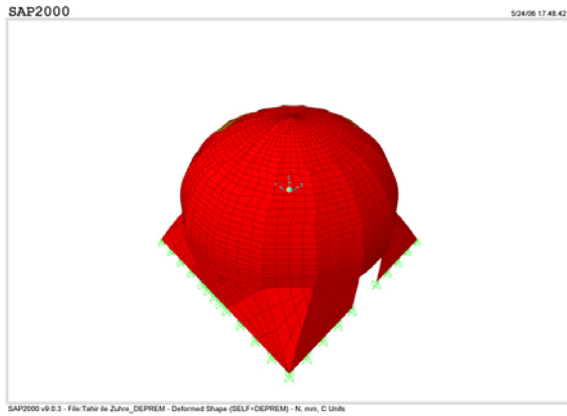


Figure 25 3D deformed shape of the upper structure of the monument under the combination of earthquake load and dead load

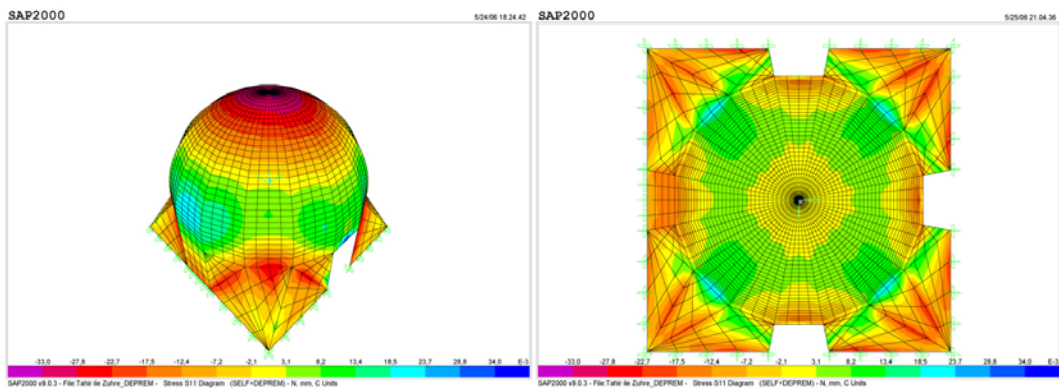


Figure 26 3D and bottom views of S11 diagram of the upper structure of the monument under earthquake load

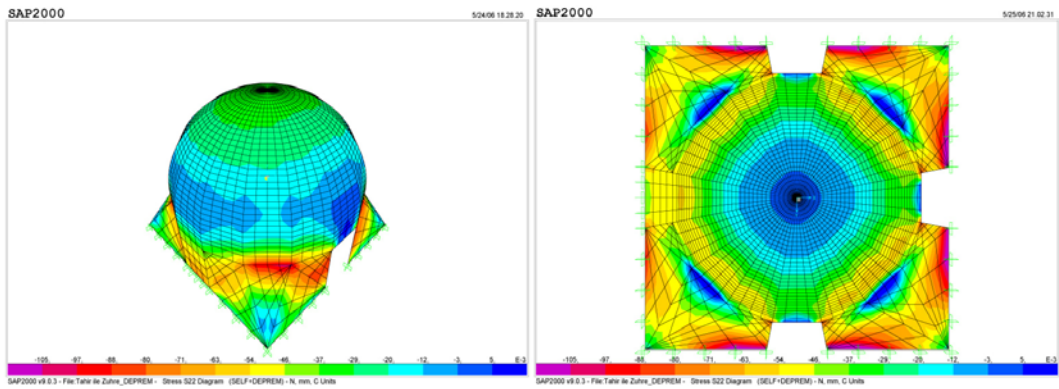


Figure 27 3D and bottom views of S22 diagram of the upper structure of the monument under earthquake load

As seen, the developing maximum tensile stress values are in the order of 0.04 MPa for S11 and 0.01 MPa for S22, which are far beyond the tensile strength, 0.4 MPa. Figure 28 and Figure 29, on the other hand, the distributions of shear stresses, S12 and S13, respectively, developing under earthquake load.

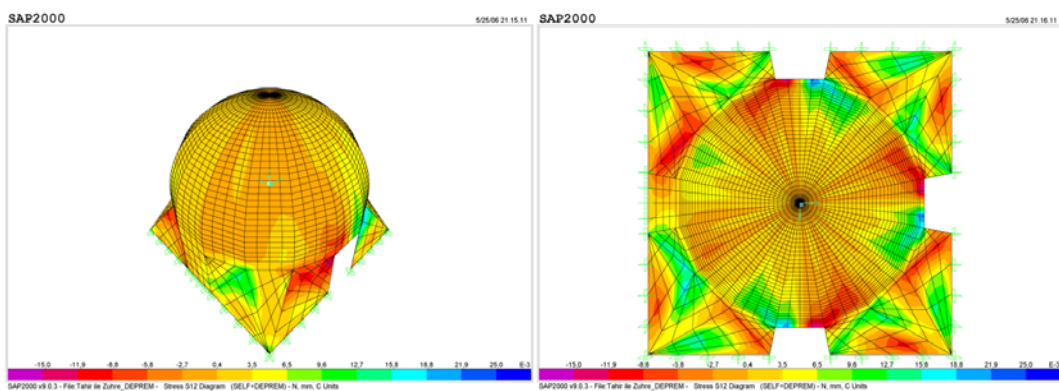


Figure 28 3D and bottom views of S12 diagram of the upper structure of the monument under earthquake load

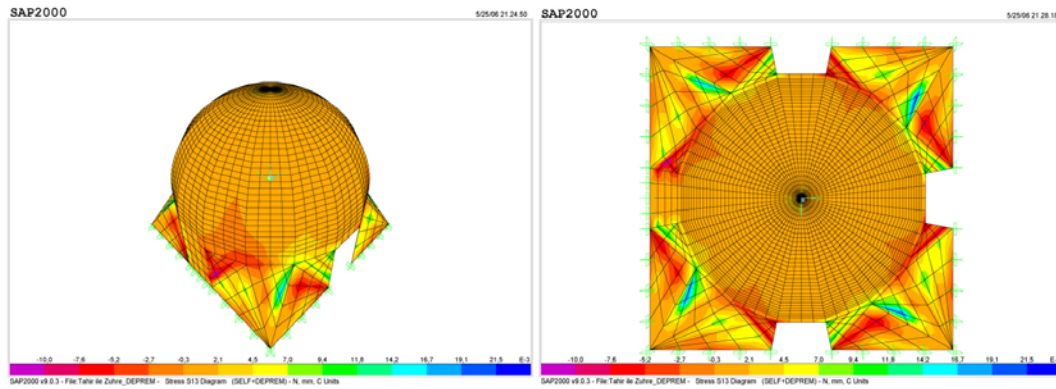


Figure 29 3D and bottom views of S13 diagram of the upper structure of the monument under earthquake load

In this study, the shear strength of the material was accepted as 1.08 MPa. Therefore, also in this case the resulting shear stress development is lower than the material could support. Also when we assume that the structure is totally wet (when the shear strength dropped to 0.86 MPa), the structure continues to appear safe.

3.6.5 Partially Collapsed Masonry Superstructure Completed Using Concrete, Analysed under Dead Load

For simulating the case that the superstructure is partially collapsed and that the missing part is completed utilizing concrete bricks, a random part (composed of 369 areas) of the previously constructed shell model with 2448 shell elements was defined to be concrete (Figure 30). The material characteristics of concrete were taken as those default at the software used for the structural analyses, SAP 2000. In this part of the study, possibility of crack formation on the original masonry structure as well as on the concrete completion was investigated. For this purpose,

the developing tensile stresses are investigated.



Figure 30 3D undeformed and deformed views of the upper structure of the monument, partially collapsed and completed using concrete, under dead load (red and blue demonstrate masonry and concrete materials, respectively)

When the constructed model was analysed under dead load, resulting maximum tensile stress distributions was as shown in Figure 30.

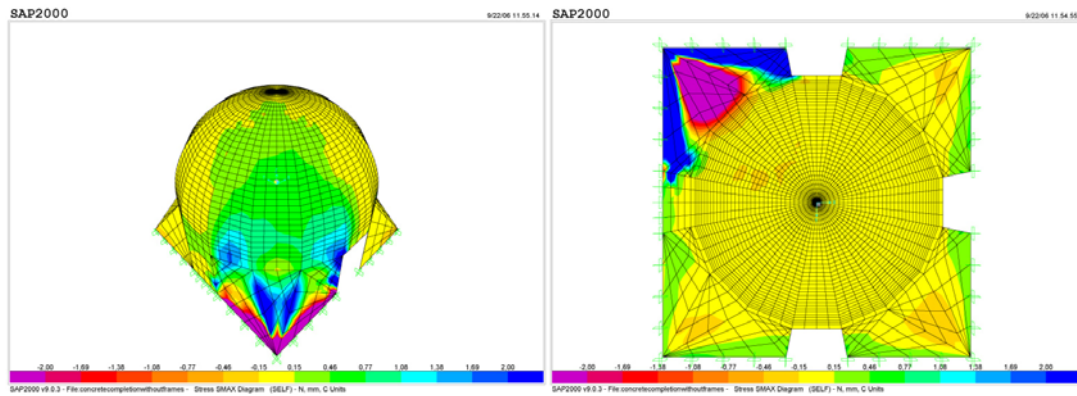


Figure 31 3D and bottom SMAX diagrams of the upper structure of the monument, partially collapsed and completed using concrete, under dead load

As can be seen in the figure, a much higher stress concentration occurred at the angle of the transition part in comparison with the other parts of the superstructure. The reason for this is that because of the geometry of the structure under investigation, at the angle a closed system of stresses occurred and it hardly affected the domed part. At the concrete part, tensile stresses exceeding 2 MPa formed. Therefore, crack formation was observed at the lower parts of then Turkish triangles, seen as dark blue in Figure 31. Moreover, would masonry material crack at the bottoms of Turkish triangles as well.

3.6.6 Partially Collapsed Masonry Superstructure Completed Using Concrete, Analysed under a Combination of Dead Load and Uniform Temperature Load of 40°C

This time, the model constructed for the previous analysis was analysed under a combination of dead load and uniformly distributed temperature load defined as a

temperature difference of 40°C. As mentioned before, the coefficients of thermal expansion of concrete and masonry material were assigned as $10 \times 10^{-6} \text{ }^\circ\text{C}^{-1}$ and $7 \times 10^{-6} \text{ }^\circ\text{C}^{-1}$, respectively. Therefore, under a temperature change the concrete material would try to change in volume differently in comparison to the masonry material generating tensile stresses. It was tried to be answered if these tensile stresses exceed the materials' tensile capacities, causing cracks.

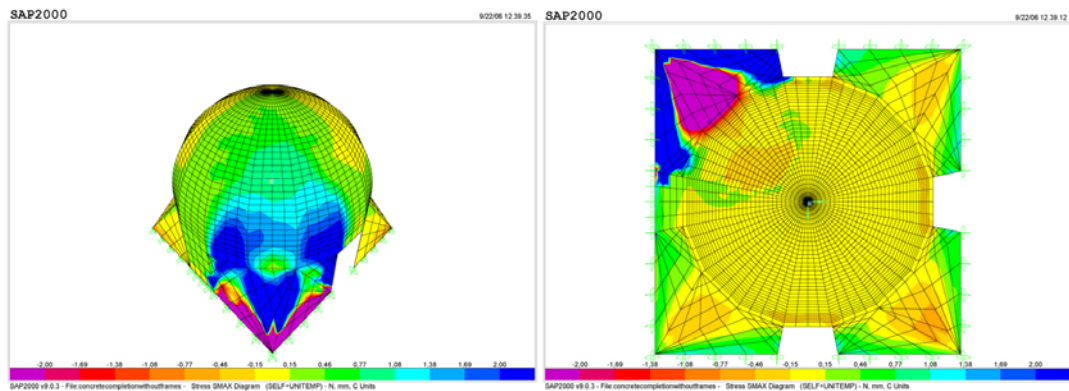


Figure 32 3D and bottom SMAX diagrams of the upper structure of the monument, partially collapsed and completed using concrete, under dead load and 40°C uniform temperature load

As seen, the concrete part is trying to expand more than masonry part, due to the difference between thermal expansion coefficients. Therefore, at the inner side of the part completed using concrete, compressive stresses are formed, while for the masonry part the situation is exactly opposite. The resulting stress formation exceeded the accepted strength value at the lower sections concrete material (the zone shown in dark blue in Figure 32). Again, here the stresses were concentrated at this part. There, the tensile stresses are in the order of 7.4 MPa, which cannot be

tolerated by concrete material in no way. Moreover, at the bottom parts of Turkish triangles the same situation was seen for masonry material. Also there the tensile intolerable stresses, close to 0.8 MPa, formed.

3.6.7 Partially Collapsed Masonry Superstructure Completed Using Concrete, Analysed under a Combination of Dead Load and Randomly Distributed Temperature Load of 25°C

To render the results more realistic and more observable in real life as sun exposure, the same model was analysed also under a randomly distributed temperature load, defined as a temperature difference of 25°C (Figure 20). The resulting maximum tensile stress distributions can be seen in Figure 33.

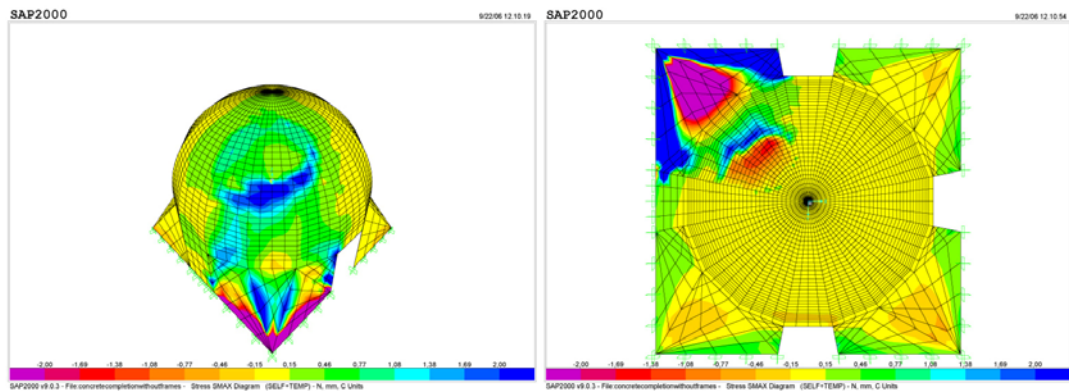


Figure 33 3D and bottom SMAX diagrams of the upper structure of the monument, partially collapsed and completed using concrete, under dead load and 25°C randomly distributed temperature load

In concrete part, as seen in dark blue, there are parts having tensile stress formations higher than 2 MPa. The crack formation is expected there. For masonry material too, the developing tensile stresses exceeded 0.4 MPa at the bottoms of the Turkish triangles. It was seen again that the intervention made with concrete to complete the partially collapsed superstructure caused structural damages not only at the added concrete part but also at the original structure.

3.6.8 10 cm Thick Concrete Coating over Superstructure Analysed under a Combination of Dead Load and Uniform Temperature Load of 40°C

For simulating the case that the superstructure is covered with a concrete coating of 10 cm in thickness, the pre-constructed shell model with 2448 shell elements was connected to another shell model covering the original dome and representing a concrete coating with 2448 areas by offsetting the present areas perpendicularly (Figure 34). The connection between two dome layers is utilized by 2563 frame element links. These links were defined as 30 cm x 30 cm steel links, without weight.

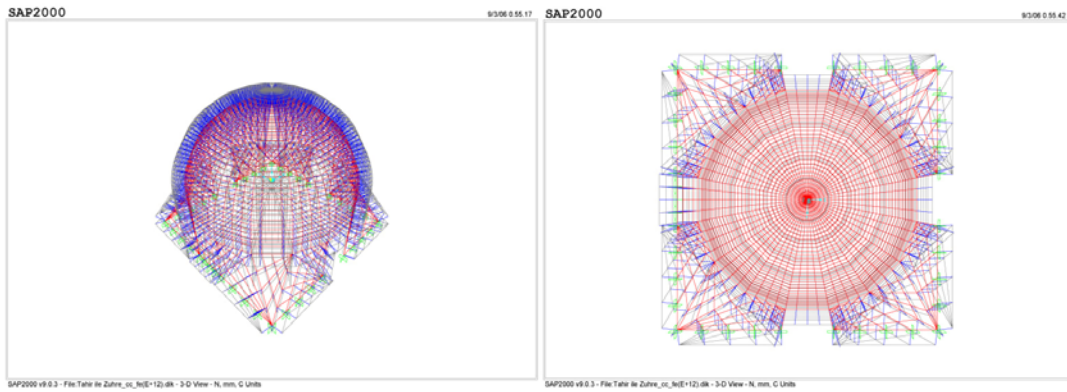


Figure 34 3D and bottom views of the upper structure of the monument composed of two layers connected with rigid links

Sensitivity analysis was performed to understand the level of fixity between two dome layers provided by the links. Sensitivity analysis of the rigid link stiffness revealed again the flexible and rigid regions of the link as a function of moment of inertia (I). Moment of inertia is the rotational inertia and describes the capacity of a cross section to resist bending. Moment of inertia for rectangular cross sections can be described mathematically as follows:

$$I = \int y^2 dA = \frac{1}{12}bh^3$$

The moment values developing on the rigid links are close to zero for low I values ($I < 1e5 \text{ mm}^4$), while moments increase and approach to a constant value for high I values ($I < 1e10 \text{ mm}^4$). The rigid link frame members become semi-rigid for $1e5 \text{ mm}^4 < I < 1e10 \text{ mm}^4$, which is therefore the sensitive region (Figure 35).

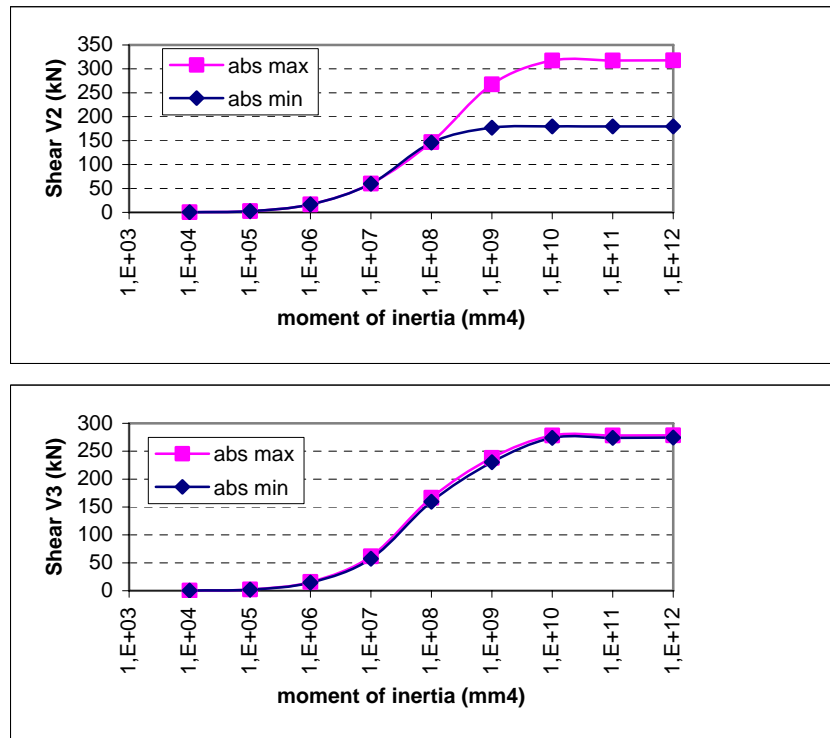


Figure 35 Graphs of minimum and maximum V2 and V3 values (i.e. shear forces in the 1-3 and 1-2 planes respectively) as a function of moment of inertia.

The tensile stress distribution in the case that the moment of inertia of frame links is equal to 10^{10} mm^4 is shown in Figure 36.

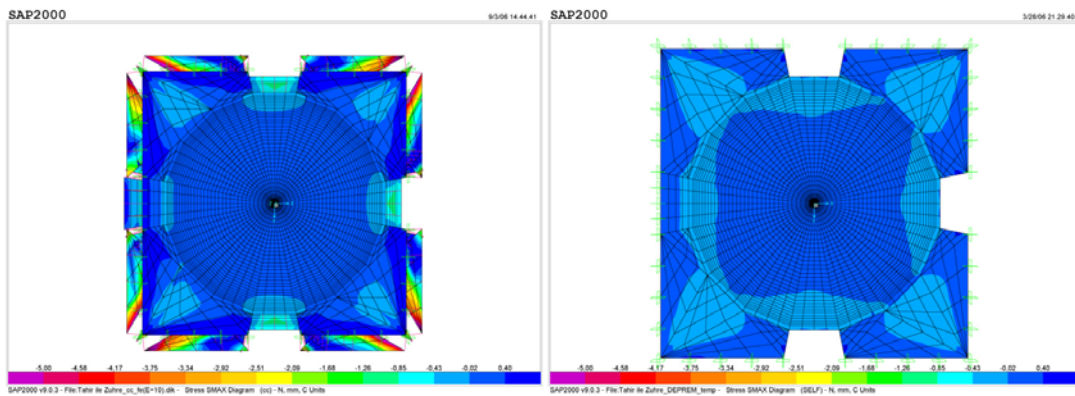


Figure 36 Bottom view of resulting SMAX diagrams of the upper structure of the monument with and without concrete cover, respectively, under dead load and uniformly distributed temperature load of 40°C for $I=10^{10} \text{ mm}^4$

Tensile stresses, resulting at the sides of window openings, in the order of 5 MPa cannot be tolerated by the cover concrete and cracking is inevitable. After the selection made according to resulting shear forces, 322 frames appeared to be critical in dry state. There were approximately 20 other critical frames if the wet shear strength was taken into consideration. Here, the delamination process in dry state was investigated. As can be seen in Figure 37, the high shear force formations were concentrated especially at the squinches. Because the squinches are rather rigid in comparison with the domed part of the superstructure. The 3D critical frame distribution is shown in Figure 38.

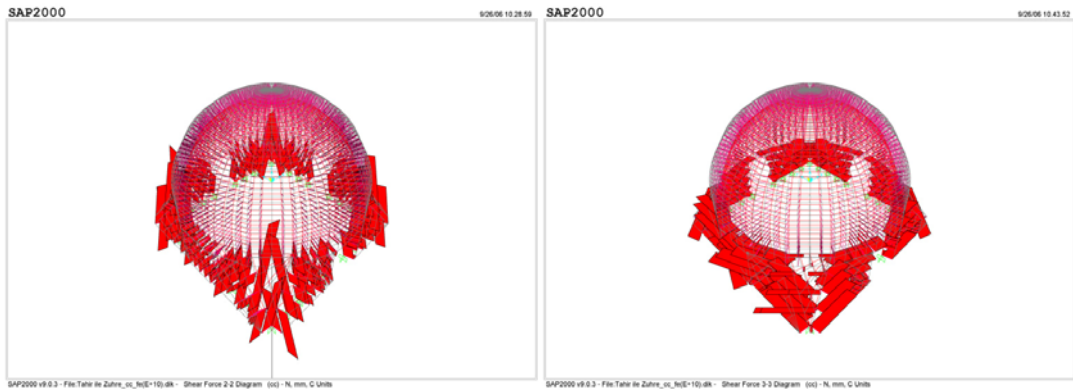


Figure 37 Graphs of resulting V2 and V3 values (i.e. shear forces in the 1-3 and 1-2 planes respectively) under dead load and uniformly distributed temperature load of 40°C for $I=10^{10} \text{ mm}^4$

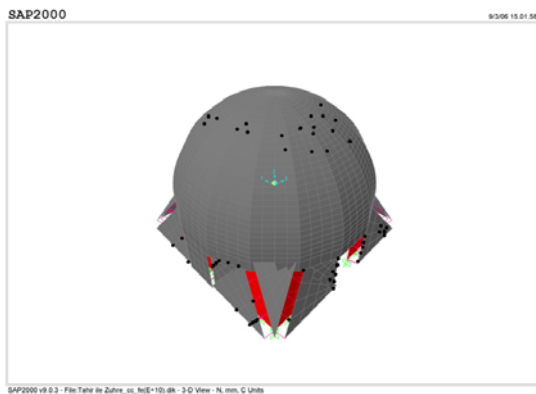


Figure 38 Critical frame elements indicated on the upper structure of the monument, covered with concrete coating, under dead load and uniformly distributed temperature load of 40°C for $I=10^{10} \text{ mm}^4$

As seen in Figure 37, excessive damage occurs in the concrete coating as well as in the original masonry structure by delamination between concrete layer and original

masonry structure. To be able to see the progress in the delamination process, the moment of inertia values of the critical frames were reduced into 10^9 mm^4 . In this case the number of critical frames were increased with 31 new critical frames. The next step in which the moment of inertia of the critical frames were reduced into 10^8 mm^4 , 293 new frames appeared to be critical.

At the end, the moments of inertia of critical frames were reduced into 10^5 mm^4 , which corresponds to the sensitive region in the resulting moment of inertia vs. shear force graph of the sensitivity analysis. The 3D and bottom views of maximum tensile stresses' distribution and 3D critical frame distribution were as follows:

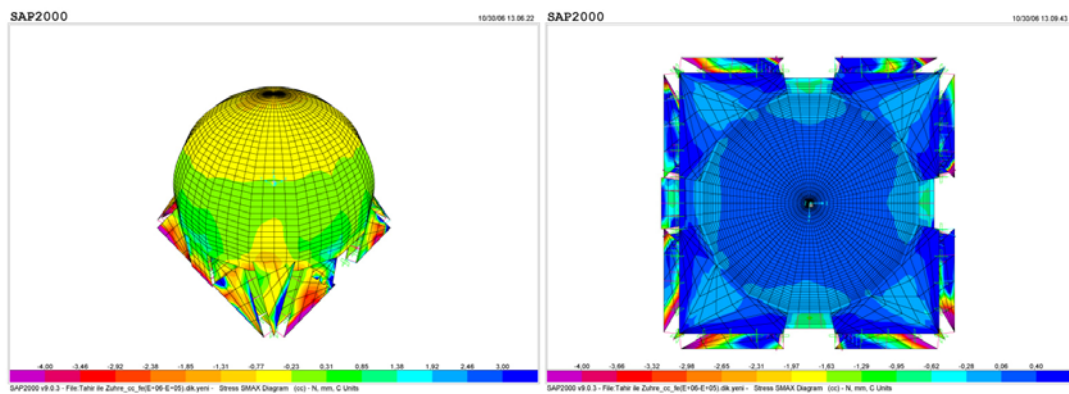


Figure 39 3D and bottom views of the SMAX diagram the upper structure of the monument covered with concrete coating, under dead load and uniformly distributed temperature load of 40°C for $I=10^5 \text{ mm}^4$

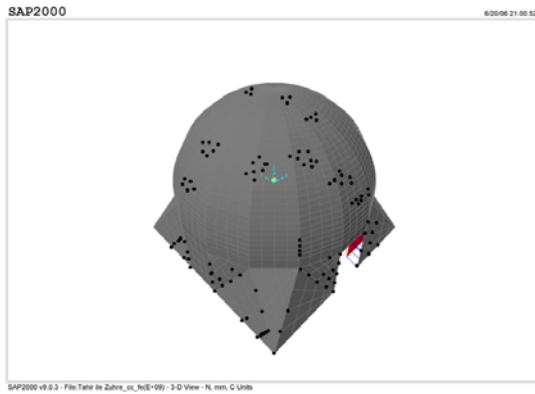


Figure 40 Critical frame elements indicated on the upper structure of the monument, covered with concrete coating, under dead load and uniformly distributed temperature load of 40°C for $I=10^5 \text{ mm}^4$

In this analysis, those were investigated: the crack development due to excessive tensile stress formation at masonry and concrete materials, and the delamination process occurring between the layers due to excessive shear stress formation at the frames. Once more, it can be seen that as a result of a wrong restoration intervention carried out using a wrong material, not only the added part is damaged but also the original structure is damaged heavily. As Figure 40 shows, at both materials cracks formed at the parts in dark blue; at the folding parts in concrete and at the bottom parts of Turkish triangles for masonry. Moreover, a delamination process would be observed at the transition zone from a squared plan to domed superstructure, provided by Turkish triangles as well as at the dome.

3.6.9 10 cm Thick Concrete Coating over Dome Only under a Combination of Dead Load and Uniform Temperature Load of 40°C

Since at the previous analysis the critical frames were appeared only at the Turkish triangles, the case that the concrete completion is realized only at the dome part of the superstructure was analysed as well. For this purpose, the pre-constructed shell model with 2448 shell elements was connected to shell model covering only the original dome and representing a concrete coating with 2112 shell elements, using 2119 rigid frames (Figure 41).

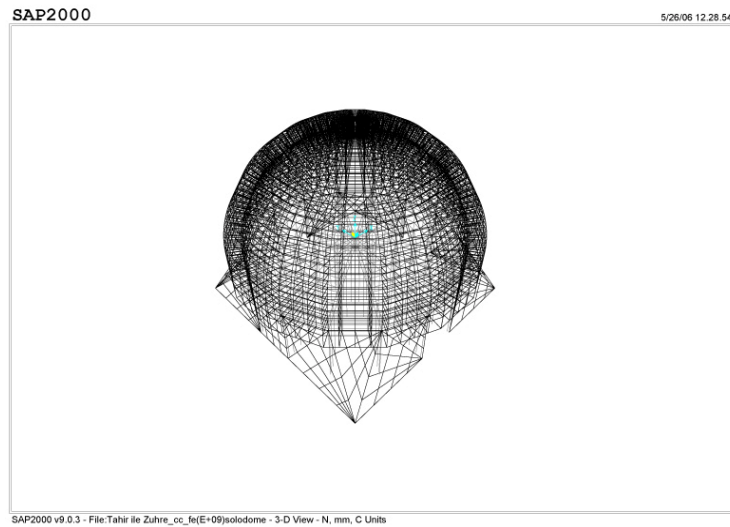


Figure 41 A 3D view of the upper structure of the monument composed of two layers connected only at the dome part with rigid links

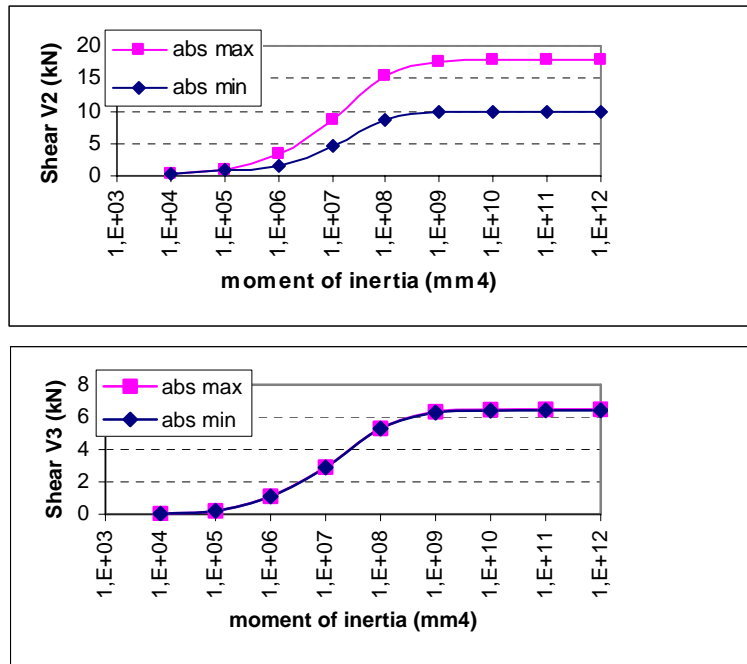


Figure 42 Graphs of minimum and maximum V2 and V3 values (i.e. shear forces in the 1-3 and 1-2 planes, respectively) as a function of moment of inertia.

As can be seen in the graphs in Figure 42, also in this case the sensitive region is the interval between $I=10^5 \text{ mm}^4$ and $I=10^9 \text{ mm}^4$. Therefore, the analysis was started with the investigation of stress level and the determination of critical frames in the case that moment of inertia is equal to 10^9 mm^4 .

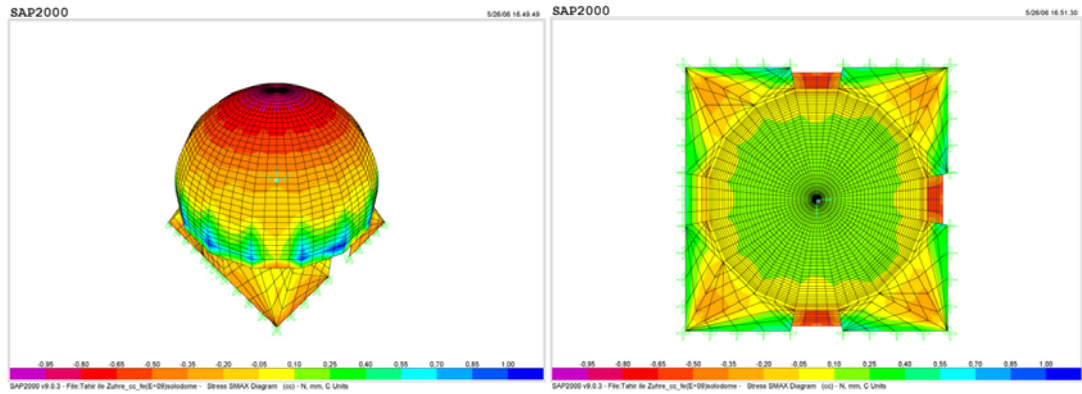


Figure 43 3D and bottom views of the SMAX diagram the upper structure of the monument, whose dome covered with concrete coating, under dead load and uniformly distributed temperature load of 40°C for $I=10^9 \text{ mm}^4$

As seen in Figure 43, the tensile stresses forming at the concrete layer is rather small in comparison with its accepted tensile strength value. Masonry material shows, however, the excessive tensile stress formation at the bottom parts of squinches. In Figure 44, this situation can be seen better. The tensile stress value reaches up to 0.6 MPa which is greater than 0.4 MPa, the accepted tensile strength for masonry material.

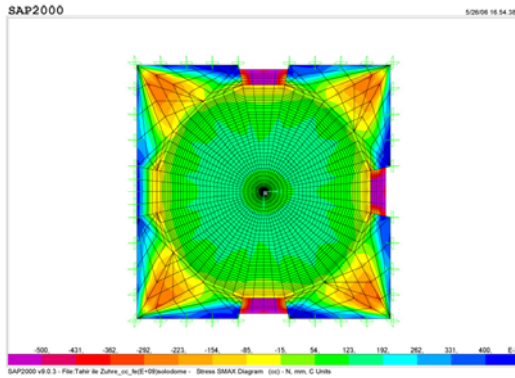


Figure 44 Bottom view of the SMAX diagram of the upper structure of the monument covered with concrete coating, under dead load and uniformly distributed temperature load of 40°C for $I=10^9 \text{ mm}^4$

Figure 45 shows the shear force graphs. According to the selection made taking the resulting shear forces into consideration, only 9 frames appeared to be critical. They all were placed at the top of the dome. Therefore, also in this case the original material got damaged and separation between layers occurred.

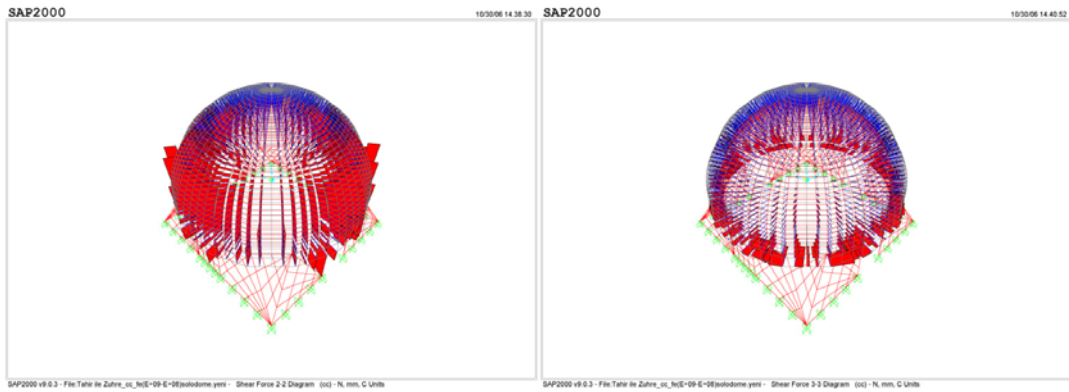


Figure 45 Graphs of resulting V2 and V3 values (i.e. shear forces in the 1-3 and 1-2 planes respectively) under dead load and uniformly distributed temperature load of 40°C for $I=10^9 \text{ mm}^4$

To follow the progress of cracking and delamination, the moment of inertia value for critical frames was changed as 10^8 mm^4 . In this case, the total number of critical frames became 10 with one new frame only.

As in the previous case, the moment of inertia value for critical frames was reduced progressively until 10^5 mm^4 . The same critical frames appeared to be critical also in this case. The 3D and bottom maximum tensile stress and critical frame distribution are shown in Figure 46 and 47.

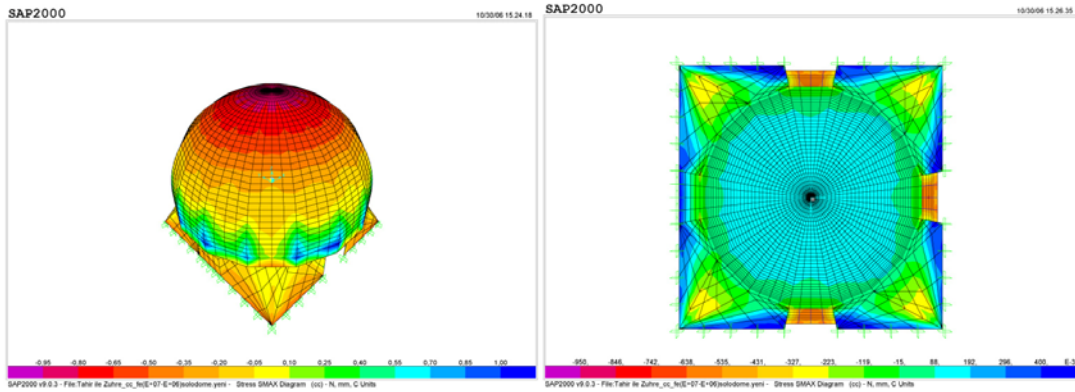


Figure 46 3D bottom views of the SMAX diagram the upper structure of the monument, whose dome covered with concrete coating, under dead load and uniformly distributed temperature load of 40°C for $I=10^5 \text{ mm}^4$

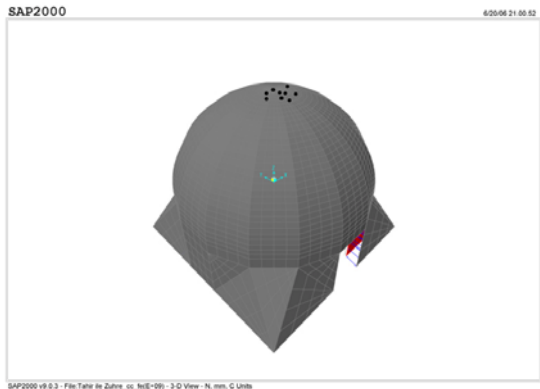


Figure 47 Critical frame elements indicated on the upper structure of the monument, whose dome covered with concrete coating, under dead load and uniformly distributed temperature load of 40°C for $I=10^5 \text{ mm}^4$

As can be seen, even in the case that the superstructure is covered only at its domed part, the crack and delamination formations occurred.

3.6.10 10 cm Thick Concrete Coating over Superstructure under a Combination of Dead Load and Randomly Distributed Temperature Load of 25°C

At this last stage of the study, to render the results more observable in real life, the same model composed of 2448 shell elements representing masonry superstructure linked, by 2563 rigid links to another 2448 shell elements representing concrete coating of 10 cm in thickness, was analyzed under a partially acting temperature load of 25 °C, again, to simulate the effect of an eventual sun exposure (Fig. 20).

Also in this case, a sensitivity analysis was carried out to see where delamination process begins. As seen in Figure 48, the sensitive region in this case was found similar to the previous study, as between $I=10^6 \text{ mm}^4$ and $I=10^9 \text{ mm}^4$.

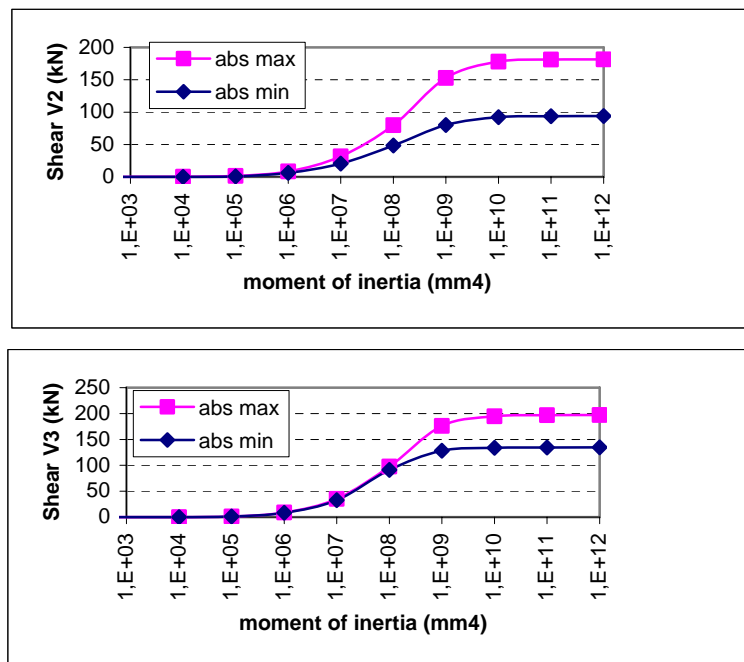


Figure 48 Graphs of minimum and maximum V2 and V3 values (i.e. shear forces in the 1-3 and 1-2 planes with square and diamond markers, respectively) as a function of moment of inertia

For the moment of inertia value equal to 10^{10} mm^4 , the resulting tensile stresses at the inner face of the masonry dome get close to 0.70 MPa, at the very bottom of the Turkish triangles at the sun exposed side (positive y direction). At the outer face, on the other hand, at the limits of the temperature application area, the resulting tensile stresses reaches to even 2.7 MPa. Therefore, cracks formed (Figure 49 and 50).

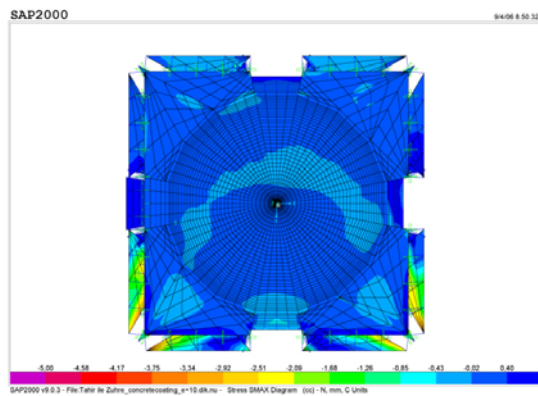


Figure 49 Bottom view of the SMAX diagram of the upper structure of the monument covered with concrete coating, under dead load and randomly distributed temperature load of 25°C for $I=10^{10} \text{ mm}^4$

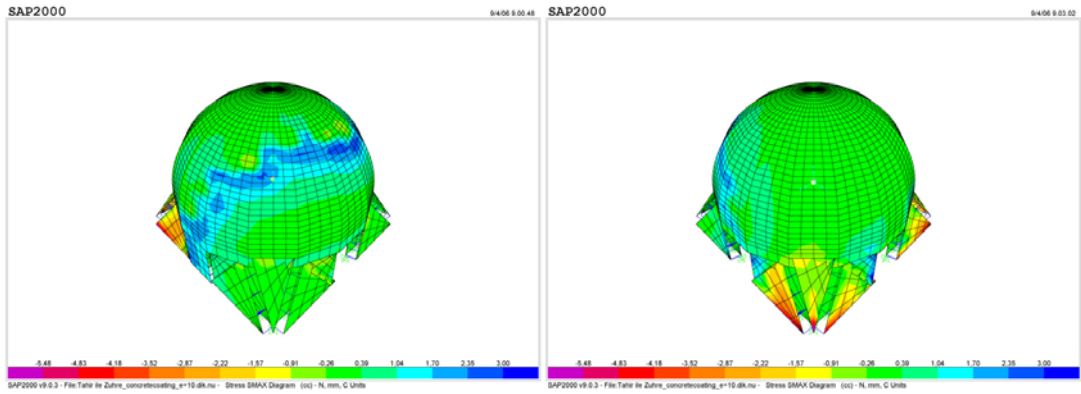


Figure 50 3D SMAX diagrams of the upper structure of the monument covered with concrete coating, under dead load and randomly distributed temperature load of 25°C for $I=10^{10} \text{ mm}^4$

The critically loaded frames were determined: they were 156 and appeared at both the zone of Turkish triangles and the dome part (Figure 45).

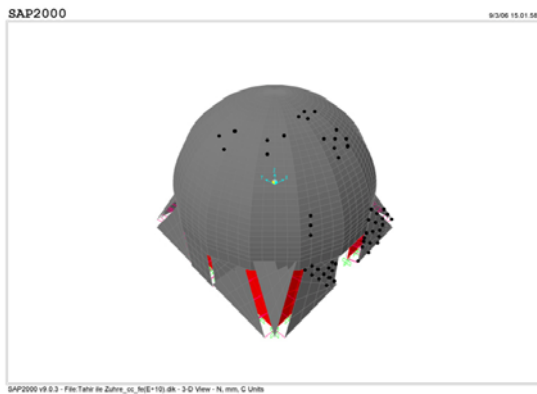


Figure 51 Critical frame elements indicated on the of the upper structure of the monument, covered with concrete coating, under dead load and randomly distributed temperature load of 25°C for $I=10^{10} \text{ mm}^4$

When the moment of inertia became 10^6 mm^4 for critical frames, maximum the tensile stress distribution is as shown in Figure 52 and the critical frame distribution is not very different from the one shown in Figure 51.

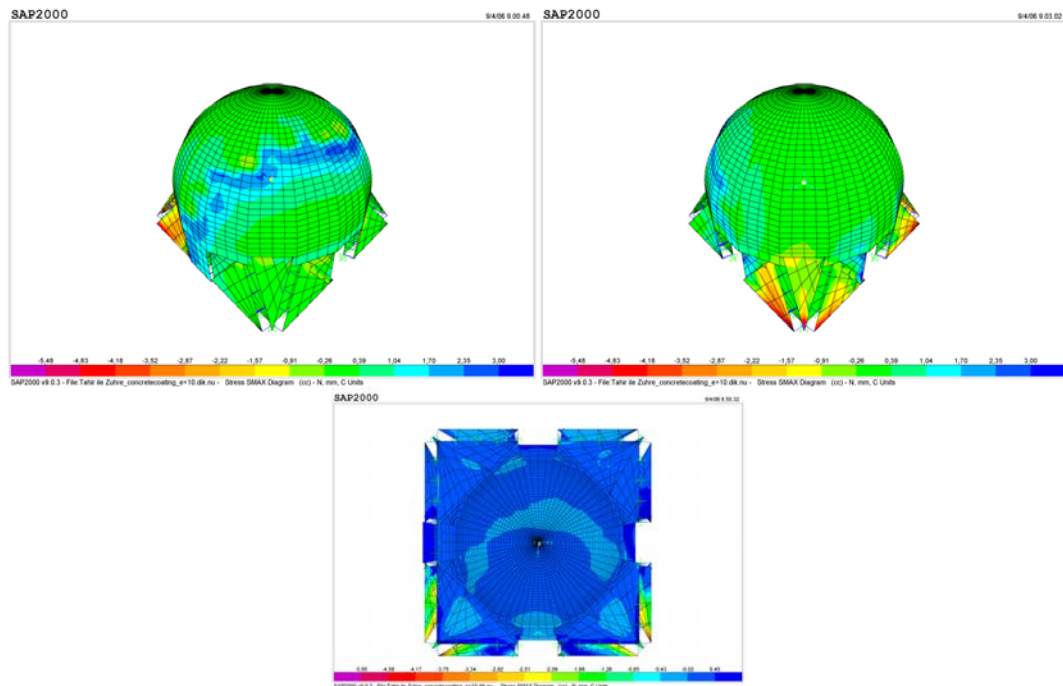


Figure 52 3D and bottom views of resulting SMAX diagrams of the superstructure covered with concrete coating, under dead load and randomly distributed temperature load of 25°C for $I_{\text{sys}}=10^7 \text{ mm}^4$ and $I_{\text{cr.frames}}=10^6 \text{ mm}^4$

As seen at the stress diagram, also in this case for masonry material, the maximum tensile stress develops at the sides of window opening in the direction of the sun exposure (positive y). For concrete cover, on the other hand, the maximum tensile stress formation occurs at the limits of the area where temperature load was applied. Therefore, concrete coating is expected to crack at the temperature gradient limits

and Turkish triangles.

As seen the resulting graphics, the separation between two layers, original masonry material and added concrete coating was intense at the Turkish triangles and at the dome at the opposite side of sun exposure. Crack formation continues too. The limits of temperature load application zone cracks totally as seen the dark blue areas in the maximum tensile stress distribution graphs. The masonry material cracks as well at the sides of the window opening in the sun exposed part. Therefore, once more, the original material is damaged as well as restoration material.

CHAPTER 4

SUMMARY AND CONCLUSION

In this study, Tahir ile Zühre Mescidi was investigated structurally in an integrated manner with its material properties. For this purpose, firstly a thorough literature survey on the brick masonry was carried out both in a material and structural level. Then, the laboratory analyses were carried out for the aim of determining basic physical, mechanical and compositional characteristics of original materials. Lastly, structural analyses was carried out with an FE model of the superstructure constructed in accordance with the actual geometry and size.

The mentioned literature survey demonstrated that there are not so many studies for the structural analyses of historic structures based on a thorough investigation of original material characteristics. In addition, that of Seljuks is one of the periods that was not investigated neither from material's point of view nor structurally. In the second part of this study in which basic physical, mechanical and compositional characteristics of the original construction materials were determined, the properties focused were: effective porosity, bulk density, water absorption capacity, modulus of elasticity, and pozzolanic activity. Effective porosity, bulk density and water absorption capacity values were determined according to the procedures suggested in RILEM, while the modulus of elasticity values of brick and mortar samples in both dry and wet states were obtained by means of ultrasonic velocity measurements. For pozzolanic activity determination of the samples, Luxan *et al.*, 1989 was taken into consideration. In addition to these properties, uniaxial compressive strength values were obtained for each sample through a correlation developed in accordance with the results of a previous study (Tuncoku, 2001).

Durability features of materials were tried to be expressed in terms of numeric values. Then, an FE model of the monument was constructed using a commercially available software, SAP 2000. The constructed model was not only analysed under loading conditions representing normal service conditions, but also two restoration interventions were tried to be simulated, i.e. partially collapsed superstructure completed with concrete and a concrete coating over it. In these simulations, temperature induced stress and strain formations were tried to be seen. At the end of this study, the conclusive comments are as follows:

- The laboratory analyses carried out in this study revealed that the construction materials, brick and mortar are very porous and are very low in bulk density (in the order of 50 % and 1.4 g/cm³, respectively). Porous and low bulk density materials are advantageous to form porous and light superstructures. Moreover, those physical properties change within a very small range in all the samples studied indicating a homogeneous superstructure i.e., a relatively uniform distribution of the materials in the superstructure in terms of mentioned characteristics.
- Brick and mortar had rather high water absorption capacity (between 29 - 40 % weight), as expected due to high porosity. High porosity and water absorption capacity could indicate good breathing property of the structure for water vapour.
- All physical properties investigated here resulted to change in a rather narrow range for each sample studied. Therefore, it can be concluded that the superstructure would response uniformly to external relevant physical phenomena (such as related deterioration, humidity content, rain etc.).
- Because the modulus of elasticity values of brick and mortar samples were determined with ultrasonic velocity measurements, the results were based on an indirect correlation rather than an experiment directly applied to the samples. For this reason, they should be considered as approximate values. The results revealed that the modulus of elasticity values of bricks changed

approximately between 680 MPa and 1880 MPa for dry state and 560 MPa and 1650 MPa for wet state. The ranges of mortars, on the other hand, were 528 MPa and 1124 MPa, for dry state and 457 MPa and 911 MPa for wet state. For most of the samples, the found values are comparable with the moduli of elasticity of other historic monuments, reported in the relevant literature, even if can be placed close to lower bound.

- Uniaxial compressive strength values of the samples were obtained through a correlation developed using previously obtained modulus of elasticity and uniaxial compressive strength values for some Seljuk mortars (Tuncoku, 2004). Calculated correlation, however, resulted in the bricks' compressive strength values too low in comparison with the values reported in the relevant literature. The reason for the low compressive strength values for bricks was thought to be related with that the correlation obtained only for mortar samples data was also used to calculate the compressive strength of the bricks. Another reason for these low values could be that the uniaxial compressive strength values had been obtained through the measurements of point load test, which normally gives relatively lower values compared to the actual strength. Average mortars' compressive strengths appeared to be lower than those of bricks and comparable with the literature values.
- In the case of masonry structures the crushing is expected to be initiated at mortar and the obtained mortar strengths, a bit lower than those of bricks, were reasonable for damage criteria. Therefore, the uniaxial compressive strength data used in this study was reasonable in spite of their lower values for brick material.
- In this study, a durability definition based on the difference between the uniaxial compressive strength values in dry and wet states was used. Most samples were appeared to have good to excellent durability. The survival of the monument for eight centuries is already a powerful indication of this high durability feature.
- Pozzolanic activity analysis of brick and mortars indicated good

pozzolanicity for all samples except one sample appeared to have no pozzolanic property. High pozzolanic activity is an indication of high bonding property between construction materials. Therefore, the homogenization process in FE modelling carried out in this study, accepting that the structure is made of a unique material whose properties is an average of the different ones was reasonable.

- Masonry is a composite material, which is commonly heterogeneous and non-linear in property. Therefore, the difficulty of investigating masonry from mechanical point of view is that even if the mechanical properties of components of masonry, i.e. brick and mortar, are determined by laboratory analyses, it is hard to extrapolate those into the strength of masonry itself. In this study, for the aim of obtaining the composite values of mechanical properties, modulus of elasticity and uniaxial compressive strength, the principle of the compatibility of deformations through Hooke's Law and European Standards (EUROCODE 6) were used, respectively. The composite values are comparable with the values reported in the relevant literature.
- For the case of an existing historic monument, the mechanical properties of brick and mortar that composes masonry should be determined through taken samples, which are normally not in sufficient in number and do not have standard test size and shape. Moreover, since masonry is not homogeneous in distribution, taking representative samples is also a difficult process. In spite of shortcomings i.e., limited number and size of the samples used in this study, the results of the laboratory analyses were consistent among each other and with the relevant literature.
- A finite element model of the superstructure was constructed and linear elastic analysis was carried out. Linear elastic analysis is enough for low deformation range as in then case here. However, nonlinear analysis would be necessary for high deformations and strains especially for masonry structures such as Tahir ile Zühre Mescidi.

- The model was constructed using shell elements and for each analysis that was carried out in this study, the same shell model was used.
- Tahir ile Zühre Mescidi is safe under normal service conditions, defined for the conditions of either dead load, snow load and wind load alone or dead load and temperature load applying simultaneously. Dead load was calculated by the program itself, using the bulk density data input to the computer program used. Snow load and wind load were calculated according to the Turkish Standards (TS 498). Temperature load defined as a difference of 25°C and applied to a randomly chosen face of the superstructure was reasonable during a summer day. Therefore, the large safety margin resulted at the end of the analyses was convincing, as the lifetime of the monument, more than eight centuries so far, demonstrates.
- The structure was appeared to be safe also under earthquake load, which was generally the governing factor for the historic structures standing for centuries under normal service conditions. The resulting stress level might be seen too low, at first sight. However, the superstructure is very bulky and shallow. It is reasonable that the stress level under earthquake load is in the same order with that under dead load, including also the earthquake acceleration amplification. The result was an indication of the large safety margin of the structure in general.
- The case that the superstructure is partially collapsed and is completed using concrete material was tried to be modelled and dead load effects were simulated. The analyses showed that tensile stress formation in both concrete and masonry materials exceeded the accepted tensile strength value. Therefore crack formation occurred at the Turkish triangles' zone for concrete and at the very bottoms of Turkish triangles for masonry.
- For the case that the superstructure is partially collapsed and completed using concrete material, an eventual crack propagation was resulted for masonry superstructure under a uniform temperature load of 40°C. Cracks formed at the sides of window openings for masonry, and at the bottoms of

the transition zone between dome and Turkish triangles for concrete.

- The analysis for the case that the superstructure is partially collapsed and completed using concrete material was repeated under a temperature load of 25°C which was applied at one side of the dome in an arbitrary manner to simulate the effect of sun exposure. Concrete material would be damaged under mentioned loading conditions through crack formations due to excessive tensile stresses. Crack formation was concluded for masonry material too; at the bottoms of the superstructure, the resulting tensile stresses exceeded the tensile strength of the material.
- The other case that was tried to be simulated is that the superstructure is covered with a concrete coating, 10 cm in thickness. For this simulation, rigid frame links were defined between concrete and masonry superstructure layers. Sensitivity analyses on rigid links stiffness were conducted in order to simulate eventual detachment between layers. Usage of rigid links together with sensitivity analysis enabled modelling of non-linear phenomenon (like detachment or slippage between layers) in a linear FE model.
- For the case that the superstructure is covered with a concrete coating, 10 cm in thickness, under a uniformly distributed temperature load of 40°C, delamination was observed heavily at the Turkish triangles and at the dome. Moreover, at the concrete layer and at the masonry dome, cracks formed, again, due to the resulting tensile stresses too high to be tolerated.
- For the case that *only the domed part* of the superstructure is covered with a concrete coating, 10 cm in thickness, crack formation was observed for masonry material at the sides of window openings. At the concrete cover, crack formation did not occur. Moreover, a delamination process at the top of the dome was concluded.
- According to the results, when the superstructure is covered with 10 cm thick concrete material, and loaded with sun exposure which creates a temperature difference of 25°C in an arbitrary face of the superstructure, a

separation process would take place between concrete and masonry materials at the Turkish triangles, in the sun exposed region. The limits of temperature load application zone would crack at the concrete coating. Moreover, masonry material would get damaged at the sides of window openings in the sun exposed region. Also in this case a big scaled separation between masonry and concrete occurred, both at the Turkish triangles and at the dome.

- Most of the analyses representing different cases of inappropriate restoration works using concrete clearly showed the formation of the structural damage at the original dome and to the concrete material itself as detachment between different materials as well as crack formation; therefore, their applications should be avoided. It should be noted that the damage would be much more when the material is wet. It is important to be able to simulate the damage occurring also in structural level for such inappropriate restoration works.
- Also in the cases that the formation of any structural damage is not observed at the end of the analyses carried out here, it should not be forgotten that concrete will always provoke degradation based on phenomena in the level of material. concrete is impermeable and its use provokes the deterioration of original material by dampness and salt crystallization. Concrete has been excluded from any eventual intervention of restoration and conservation of historic structures and it should not be used in no condition.
- Nearly all masonry spanning elements, including domes, have rather large margin of safety because of their stable geometry. In this study, only the domed superstructure of the structure was studied and the resulting safety margin was concluded also for this, which is more than 13 for dead load.
- As mentioned before, when the material properties of masonry material are to be determined through laboratory analyses, the samples are normally not in sufficient amount, and they do not have standard test size and shape. Moreover, since masonry is a highly heterogeneous material, taking

representative samples is also a difficult task. Therefore, the laboratory analyses should be supported by *in situ* investigations, whenever possible.

- The Anatolian Seljuk period, in spite of the large architectural heritage they had left behind, has not been investigated deeply so far, neither in terms of their construction materials' nor construction techniques' point of view. Therefore, with the resulting information obtained from this study, the necessity to enlarge the extent of the study to more whole Anatolian Seljuk Period structures, together with a more extensive material survey is noted. This study has provided some understanding about the subject and has the quality of beginning.
- This study clearly showed that to carry out a restoration work, the structure should be recognized well, both in terms of materials' and structural point of views. Only in this case, the interventions can provide the desired effect.

REFERENCES

- ABYYHY; Afet Bölgelerinde Yapılacak Yapılar Hakkında Yönetmelik (Specifications for Structures to be Built in Disaster Areas)
- ASTM D 2845-90; Standard Test Method for Laboratory Determination of Pulse Velocities and Ultrasonic Elastic Constants of Rock
- AKMAYDALI, H.; Konya-Merkez Tahir ile Zühre Mescidi; Rölöve Restorasyon Dergisi, 3; 1982; 101-121
- ASLANAPA, O.; Turkish Art and Architecture; London; Praeger Publishers;1971
- ATÇEKEN, Z.; Konya'daki Selçuklu Yapılarının Osmanlı Devrinde Bakımı ve Kullanılması; Ankara; Türk Tarih Kurumu; 1998
- BAKIRER, Ö.; "Anadolu Selçuklularında Tuğla İşçiliği"; Türk Tarih Kurumu Basımevi, Ankara; 1972
- BAKIRER, Ö.; Selçuklu Öncesi ve Selçuklu Dönemi Anadolu Mimarisinde Tuğla Kullanımı; Ankara; METU; 1981
- BAKIRER, Ö.; "Study on the Use of Brickbonds in Anatolian Seljuk Architecture"; METU Journal of the Faculty of Architecture; vol 6, no 2; 1994; 143-181
- BAKIRER, Ö.; "Anadolu Selçuklu Mimarisinde Yapı Malzemeleri"; IV. Milli Selçuklu Kültür ve Medeniyeti Semineri Bildirileri - Ayrı Basım; Konya; 1995; 165-181
- BARONIO, G., BINDA, L.; "Study of the Pozzolanicity of Some Bricks and Clays"; Construction and Building Materials 11; 1997; 41-46
- BERNARDESCHI, K., PADOVANI, C., PASQUINELLI, G.; "Numerical Modelling of the Structural Behaviour of Buti's Bell Tower"; Journal of Cultural Heritage 5; 2004; 371-378
- BINDA, L., ANZANI, A.; "Structural Behaviour and Durability of Stone

Masonry”; Saving Our Architectural Heritage: The Conservation of Historic Stone Structures; Ed. Bear, N.S., Snethlage, R.; John Wiley and Sons Ltd.; 1997

- BINDA, L., SAISI, A., TIRABOSCHI, C.; “Investigation Procedures for the Diagnosis of Historic Masonries”; Construction and Building Materials 14; 2000; 199-233
- BINDA, L., SAISI, A., ZANZI, L.; “Sonic Tomography and Flat-Jack Tests as Complementary Investigation Procedures for the Stone Pillars of the Temple of S. Nicolò l’Arena (Italy)”; NDT&E International 36; 2003; 215-227
- BUGINI, R., SALVATORI, A., CAPANNESI, G., SEDDA, A.F., D’AGOSTINI, C., GIULIANI, C.F.; “Investigation of the Characteristics and Properties of ‘Cocciopesto’ from the Ancient Roman Period”; *Conservation of Stone and Other Materials*, Proceedings of the International UNESCO-RILEM Congress; Thiel, M.J.; Paris; 1993
- CARPINTERI, A., INVERNIZZI, S., LACIDOGNA, G.; “In Situ Damage Assessment and Nonlinear Modelling of a Historical Masonry Tower”; Engineering Structures 27; 2005; 387-395
- CLUNI, F., GUSELLA, V.; “Homogenization of Non-Periodic Masonry structures”; International Journal of Solids and Structures 41; 2004; 1911-1923
- CORRADI, M., BORRI, A., VIGNOLI, A.; “Experimental Study on the Determination of Strength of Masonry Walls”; Construction and Building Materials 17; 2003; 325-337
- ÇAKMAK A. S., MOROPOULOU A., MULLEN C. L.; “Interdisciplinary Study of Dynamic Behaviour and Earthquake Response of Hagia Sophia”; Soil Dynamics and Earthquake Engineering 14; 1995; 125-133
- DAVEY, N., A History of Building Materials, Phonix House, London, 1961
- DİLAVER, S.; “Anadolu’da Tek Kubbeli Selçuklu Mescidlerinin Mimarlık Tarihi Yönünden Önemi”; Sanat Tarihi Yıllığı; 1970; 17-28

- DÜLGERLER, O.N.; “Konya’nın Dünü ve Bugünü”; Konya; Ed. Halıcı, F.; Ankara; Güven Matbaası; 1984
- ERSOY, U.; Reinforced Concrete; Ankara; Middle East Technical University; 1994
- GIAMBANCO G., RIZZO S., SPALLINO R.; “Numerical Analysis of Masonry Structures Via Interface Models”; Computer Methods in Applied Mechanics and Engineering 190; 2001; 6493 - 6511
- GIORDANO, A., MELE, E., DE LUCA, A.; “Modelling of Historical Masonry Structures: Comparison of Different Approaches Through a Case Study”; Engineering Structures 24; 2002; 1057-1069
- GIULIANI C.F.; L’Edilizia nell’Antichità; La Nuova Italia Scientifica; Roma; 1990
- GUINEA, G.V., HUSSEIN, G., ELICES, M., PLANAS, J.; “Micromechanical Modelling of Brick-Masonry Fracture”; Cement and Concrete Research 30; 2000; 731-737
- HENDRY, E.A.W.; “Masonry Walls: Materials and Construction”; Construction and Building Materials 15; 2001; 323-330
- HEYMAN, J.; The Masonry Arch; Ellis Horwood Limited; England; 1982
- HEYMAN, J.; The Stone Structure – Structural Engineering of Masonry Architecture; Cambridge University Press; United Kingdom; 1995
- KATOĞLU, M.; 13. Yüzyıl Konyasında Bir Cami Grubunun Plan Tipi ve “Son Cemaat Yeri”; Türk Etnoğrafya Dergisi, 9; 1966; 81-100
- KONYALI, İ.H.; Abideleri ve Kitabeleri ile Konya; Konya; Yeni Kitap Basımevi; 1964
- KUBAN, D.; Selçuklu Çağında Anadolu Sanatı; İstanbul; Yapı Kredi Yayınları-1567; 2002
- KURAN, A.; “Anatolian-Seljuk Architecture”; The art and Architecture of Turkey; Ed. Akurgal, E.; U.S.A; Rizzoli International Publications, Inc.; 1980

- LOURENÇO, P.B.; “Assessment, Diagnosis and Strengthening of Outeiro Church, Portugal” *Construction and Building Materials* 19; 2005; 634-645
- LU, M., SCHULTZ, A.E., STOLARSKI, H.K.; “Application of the Arc-Length Method for the Stability Analysis of Solid Unreinforced Masonry Walls Under Lateral Loads”; *Engineering Structures* 27; 2005; 909-919
- LUXAN, M.P., MADRUGA, F., SAAVEDRA, J.; “Rapid Evaluation of Pozzolanic Activity of Natural Products by Conductivity Measurements”; *Cement and Concrete Research* 19; 1989; 63-68
- MAINSTONE, R.J.; “Characteristics and Assessment of Old Masonry Structures”; *Structural Conservation of Stone Masonry – International Technical Conference*; Athens; 1989; 63-76
- MARTINI, K.; “Ancient Structures and Modern Analysis: Investigating Damage and Reconstruction at Pompeii”; *Automation in Construction* 8; 1998; 125-137
- MELE, E., De LUCA, A., GIORDANO, A.; “Modelling and Analysis of a Basilica under Earthquake Loading”; *Journal of Cultural Heritage* 4; 2003; 355-367
- MOROPOULOU, A., BISCONTIN, G., BAKOLAS, A., BISBIKOU, K.; “Technology and Behaviour of Rubble Masonry Mortars”; *Construction and Building Materials* 11; 1997; 119-129
- MOROPOULOU, A., CAKMAK, A.S., LOHVYN, N.; “Earthquake Resistant Construction Techniques on Byzantine Monuments in Kiev”; *Soil Dynamics and Earthquake Engineering* 19; 2000; 603-615
- MOROPOULOU, A., CAKMAK, A.S., BISCONTIN, G., BAKOLAS, A., ZENDRI, E.; “Advanced Byzantine Cement Based Composites Resisting Earthquake Stresses: the Crushed Brick / Lime Mortars of Justinian’s Hagia Sophia”; *Construction and Building Materials* 16; 2002; 543-552
- MOROPOULOU, A., CAKMAK, A.S., LABROPOULOS, K.C., VAN GRIEKEN, R., TORFS, K.; “Accelerated Microstructural Evaluation of a Calcium-Silicate-Hydrate (C-H-S) Phase in Pozzolanic Pastes Using Fine

- Siliceous Sources: Comparison with Historic Pozzolan Mortars”; Cement and Concrete Research 34; 2004; 1-6
- MOROPOULOU, A., BAKOLAS, A., ANAGNOSTOPOULOU, S.; “Composite Materials in Ancient Structures”; Cement & Concrete Composites 27; 2005; 295-300
 - MUNSELL BOOK OF COLOUR; Munsell Colour Company, Inc.; Baltimore, Maryland; 1966
 - O’DWYER D.; “Funicular Analysis of Masonry Vaults”; Computers and Structures 73; 1999; 187-197
 - PLUMRIDGE, A., MEULENKAMP, W.; Brickwork: Architecture and Design; Breslich & Foss, London; 1993
 - RAMOS, L.F., LOURENÇO, P.B.; “Modelling and Vulnerability of Historical City Centers in Seismic Areas: a Case Study in Lisbon”; Engineering structures 26; 2004; 1295-1310
 - RILEM; Tentative Recommendations, Commission-25-PEM, Recommended Tests to Measure the Deteriorated Stone and to Assess the Effectiveness of Treatment Methods, Matériaux and Construction 13; 1980; 173-253
 - SAP 2000® Three Dimensional Static and Dynamic Finite Element Analysis and Design of Structures, Advanced 9.0.3; Computers and Structures Inc.; Berkeley, California, USA
 - TEUTONICO, J.M.; A Laboratory Manual for Architectural Conservators; ICCROM, Rome; 1988; 32-122
 - TS 498, Yapı Elemanlarının Boyutlandırılmasında Alınacak Yüklerin Hesap Değerleri (Design Loads for Buildings); Türk Standartları Enstitüsü; 1987
 - TS EN 196-5, Çimento Deney Metotları- Puzolanik Çimentolarda Puzolanik Özellik Tayini Methods of testing cement-Part 5: Pozzolanicity test for pozzolanic cement; Türk Standartları Enstitüsü; 2002
 - TS ENV 1996-1-1, Kagir Yapıların Tasarımı- Bölüm 1-1: Binalar İçin Genel Kurallar- Donatılı ve Donatısız Kagir Kuralları (Design of Masonry Structures – Part1-1: General Rules for Buildings – Rules for Reinforced

and Unreinforced Masonry) (EUROCODE 6); Türk Standartları Enstitüsü; 2001

- TUNCOKU, S.S.; The Restoration Project of a XIIIth Century Anatolian Seljuk “Mescid” in Konya with the Emphasis on the Materials and Related Problems; Unpublished Master Thesis, Restoration Program; METU; 1993
- TUNCOKU, S.S.; Characterization of Masonry Mortars Used in Some Anatolian Seljuk Monuments in Konya, Beyşehir and Akşehir; Unpublished Ph.D Thesis, Restoration Program; METU; 2001
- ÜNAY, A.İ.; Tarihi Yapıların Depreme Dayanımı; METU; 2002
- VALUZZI, M.R., BONDI, A., da PORTO, F., FRANCHETTI, P., MODENA, C.; “Structural Investigation and Analyses for the Conservation of the ‘Arsenal’ of Venice”; Journal of Cultural Heritage 3; 2002; 65-71
- WINKLER, E.M.; Durability Index of Stone; Bulletin of Association of Engineering Geologist 23; 1986; 344
- ZUCCHINI, A., LOURENÇO, P.B.; “A Micro-Mechanical Model for the Homogenisation of Masonry”; International Journal of Solids and Structures 39; 2002; 3233-3255
- ZUCCHINI, A., LOURENÇO, P.B.; “The Coupled Homogenization-Damage Model for Masonry Cracking”; Computers and Structures 82; 2004; 917-929